

## Replies to Reviewer #1 Comments/suggestions

**General comments:** The manuscript shows the distribution of clouds in different seasons over the Indian radiosonde station of Gadanki. A long term series of radiosonde measurements has been used for evaluating the cloud base and top heights and the cloud thickness. The study is interesting in terms of methodological approach and results. The manuscript is well written and structured.

**Reply:** First of all we wish to thank the reviewer for going through the manuscript carefully, appreciating actual content of the manuscript and providing constructive comments/suggestions which made us to improve the manuscript content further.

### Specific Comments:

1. Assuming that the methodology performs well for detecting the cloud base and top, the results are very promising. However, it could be useful a comparison with other measurements for validating the results: e.g. CALIPSO/Cloudsat for cloud tops, and/or ground based lidars for cloud base. I probably did not understand what the authors want to show with Figure 8 because it looks like the values are not consistent with those ones in Figures 6-7. Looking at Figures 6-7 the percentage of occurrences of cloud base and top heights during the monsoon season should be higher at higher altitudes than the other seasons (same for the cloud thickness).

**Reply:** At measurement location, we have Boundary Layer Lidar and Mie Lidar. When there is occurrence of multi-layer configuration BLL does not give accurate cloud base altitude for higher layers. Whereas, Mie LIDAR gives the vertical structure of the cirrus clouds (occur at higher altitude). In the present study, Cloud Vertical Structure is examined only up to 12.5 km altitude as the accuracy in RH measurements is poor at higher altitudes. Also, Mie LIDAR is operated mostly during cloud free conditions (only during cirrus cloud or clear sky conditions). Further, the timings of Radiosonde and LIDAR measurements are different. Hence we did not do inter comparison study with ground based LIDAR observations.

On the other hand, CLOUDSAT/CALIPSO overpasses over experiment location are around 02 LT and 14 LT. Whereas regular radiosonde launches are around 1730 LT. Hence, we did not do inter comparison study between regular radiosonde and CLOUDSAT/CALIPSO measurements. However, we have three hourly radiosonde observations for continuous three days in every month during Tropical Tropopause Dynamics (TTD) campaigns. Unfortunately, we did not get collocated (space and time) measurements from CLOUDSAT/CALIPSO and Radiosonde during these campaigns. (Line 227 - 240)

Figure 8 describes the CVS (Cloud base, Cloud top and cloud thickness) distribution with height observed over Gadanki location with long-term (11 years) radiosonde data at 1730 LT. From this we can understand the percentage occurrence of cloud base/cloud top of a cloud layer from all cloud configurations (Single-, multi-layer clouds). Whereas Figure 6 and 7 are diurnal variations in one-layer and two-layer clouds obtained using Tropical Tropopause Dynamics (TTD) campaigns data. During these campaigns, the radiosondes were launched every

three hourly for continuous three days in each month during Dec. 2010 to Mar. 2014. Hence the results from Figure 6 and Figure 7 need not be consistent with Figure 8.

#### Technical corrections

1. Please write always water vapor or water vapour in the whole paper

Reply: Corrected.

2. line 72 »> CVS is

Reply: Corrected. (Line 73)

3. line 161 »> were launched every three hourly for 72 hour ??

Reply: Corrected.

“During these campaigns, the radiosondes were launched every three hourly for continuous three days in each month during Dec. 2010 to Mar.2014 except in Dec. 2012, Jan., Feb., Apr., 2013”.(Line 163 – 165)

4. line 252 »> 375ma.m.sl.??

Reply: Corrected. (Line 269)

5. line 266 »> Figure4a-d

Reply: Corrected. (Line 283)

6. lines 270-289 »> In the caption of Figure 4 is reported that the values are anomalies, however in the text it looks like the authors are talking about absolute values. Can you please clarify it?

Reply: In Figure 4 only temperature is shown as anomalies (Figure 4a) and remaining parameters namely, Relative humidity, Zonal and Meridional winds are absolute values. As per reviewer suggestion the corrections are made in the text (Line 281-287).

7. line 320 »> Figure 6 (a-d) describes

Reply: Corrected. (Line 338)

8. line 525 »> CVS has already been defined

Reply: Since it is in the beginning of summary, we want to define CVS again.

We once again thank the reviewer for providing detailed comments/suggestions for betterment of the manuscript.

---END---

## Replies to Reviewer #2 Comments/suggestions

**General comments:**In the present study, the authors report the long-term GPS-sonde observations of vertical structure of clouds over a tropical station in terms of cloud base and top altitude and frequency of occurrence of single and multi-layer clouds. Diurnal and seasonal variability of vertical cloud structure are discussed. The modification of vertical thermal structure of troposphere and lower stratosphere by the presence of multi-layer clouds is also addressed. The topic of the present study is of interest to climate scientists as representation of vertically resolved clouds and their feedback in the climate models remains as one of the major sources for uncertainty. However, the present study has limitations in vertically resolving the clouds and thus in identifying the multi-layer clouds. This should be discussed in details. I recommend this manuscript for publication in ACP after a suitable revision by the authors.

**Reply:** First of all we wish to thank the reviewer for going through the manuscript carefully, appreciating actual content of the manuscript and providing constructive comments/suggestions which made us to improve the manuscript content further.

### Specific Comments:

1. Earlier results from Gadanki have shown that during the Indian summer monsoon, this location is dominated by high-altitude cirrus clouds in the height region of 14-17 km. Given the fact that the radiosonde measurements of humidity are not valid at these altitudes, the frequency of occurrence of multi-layer clouds will be underestimated, especially during monsoon. Authors should discuss this aspect with sufficient details as it has greater implication on the present results.

**Reply:** Note that the RH measurements are valid above the 12.5 km but the accuracy of RH measurement above 12.5 km altitude is ~ 7%. Using Radiosonde measurements we have also checked the cloud vertical structure till 18 km altitude. There is no significant difference in the results. These aspects are mentioned in the manuscript. (Line 403 - 405)

2. The authors claim that cloud layer boundaries detected in the present study are accurate by comparing the radiosonde detected cloud layers with that of Cloud Particle Sensor. By carefully examining this comparison shown in figure 2, one can note that there are no cloud particle at all in the detected cloud layers 2 and 4. Are they falls detection? This has important implication in estimating the frequency of occurrence of multi-layer clouds. The authors have to address this aspect.

**Reply:** There are no problems in detecting cloud layers. Absent of cloud particle concentration in layers 2 and 4 could be due to the limitations of the Cloud Particle Sensor (CPS) Sonde. One can see the thickness of the lower layers is relatively small. Hence the CPS Sonde may not have sufficient time to sample the cloud layer and hence the number concentration either low or none. We have only two cases of simultaneous measurements of Radiosonde and CPS Sonde from Gadanki location. Hence, the comparison of cloud number concentration and CVS structure is qualitative. We may need more number of simultaneous observations for further study.

3. If authors can validate their radiosonde observations of CVS using micro-pulse lidar or ceilometer, the present study will be more credible as compared to earlier studies.

**Reply:** At measurement location, we have Boundary Layer Lidar and Mie Lidar. When there is occurrence of multi-layer configuration BLL does not give accurate cloud base altitude for higher layers. Whereas, Mie LIDAR gives the vertical structure of the cirrus clouds (occur at higher altitude). In the present study, Cloud Vertical Structure is examined only up to 12.5 km altitude as the accuracy in RH measurements is poor at higher altitudes. Also, Mie LIDAR is operated mostly during cloud free conditions (only during cirrus cloud or clear sky conditions). Further, the timings of Radiosonde and LIDAR measurements are different. Hence we did not do inter comparison study with ground based LIDAR observations.

On the other hand, CLOUDSAT/CALIPSO overpasses over experiment location are around 02 LT and 14 LT. Whereas regular radiosonde launches are around 1730 LT. Hence, we did not do inter comparison study between regular radiosonde and CLOUDSAT/CALIPSO measurements. However, we have three hourly radiosonde observations for continuous three days in every month during Tropical Tropopause Dynamics (TTD) campaigns. Unfortunately, we did not get collocated (space and time) measurements from CLOUDSAT/CALIPSO and Radiosonde during these campaigns. (Line 227 - 240)

4. Using figure 3, authors claim that the cloudiness is uniform around 50 km of Gadanki. However, this figure will not serve the purpose as it is a mean of 11 years. On a given day of the radiosonde observation, the cloud cover scenario may be entirely different. Except during the Indian summer monsoon, uniform cloud cover may not be present on most of the days. Authors can discard this figure as it is not serving its purpose.

**Reply:** Figure 3(a-d) describes the seasonal mean distribution of OLR around Gadanki location at 1730 LT (around the time of radiosonde observations) obtained during pre-monsoon, monsoon, post-monsoon and, winter seasons averaged during 2006 – 2017. Since it is the mean of 11 years, we agree with reviewer that the cloud scenario on the day of the radiosonde might be different. But this is true only during pre-monsoon season and for other three seasons the climatological mean still serves the purpose. For this we have referred the visual inspection parameter from Radiosonde launch log book. Hence we would like to retain the Figure 3(a-d).

5. The explanation of diurnal variability of clouds is vague. The authors explain on the basis of interaction of short-and long-wave fluxes with clouds. The authors claim that in two-layer clouds during noon-time, the upper level cloud will be thinner due to solar heating and lower level cloud will be thicker due to long-wave heating from the ground. But figure 7(b) at ~14 hours shows the other way. Can authors explain this discrepancy? The thickness of the upper level clouds at 14 LT is comparable with that of 2 and 5 LT.

**Reply:** We mentioned that the thickness of top layer and bottom layer of two-layer clouds reaching a minimum value between 11 – 14 LT not exactly 14 LT. Also, the thickness of the top layer and bottom layer need not reduce at the same time.

- 184  
185  
186  
187  
188  
189  
190
6. Why there are no deep convective clouds at all in the single and multi-layer clouds in figure 6 and 7?

**Reply: Among the four classifications of the clouds, the percentage of occurrence of deep convective clouds is only 2% (Please see Line 423 and Figure 9d). Hence deep convective clouds are not seen in Figure 6 and Figure 7.**

- 191  
192  
193  
194  
195  
196
7. As mentioned by the authors, Das et al. (2017) using CloudSat observations reported that the peak in occurrence of cloud base and top altitude are 14 and 17 km. This will be completely missed by the present analysis as mentioned earlier. How the authors will justify their results, which will be misleading. Authors at least should mention using other sources that what fraction of clouds will be underestimated by the present analysis.

**Reply: Note that the RH measurements are valid above the 12.5 km but the accuracy of RH measurement above 12.5 km altitude is ~ 7%. Using Radiosonde measurements we have also checked the cloud vertical structure till 18 km altitude. There is no significant difference in the results. These aspects are mentioned in the manuscript. (Line 403 - 405)**

- 201  
202  
203  
204  
205  
206  
207
8. In figure 9, the authors show that the frequency of occurrence of high level clouds during winter is more than that during post-monsoon and comparable with that of monsoon. But the mid-and upper troposphere is very dry during winter as shown in figure 4(b). What is the reliability of this observation? Can authors check their analysis or provide a reference showing large occurrence of high level clouds during winter.

**Reply: The percentage occurrence of low, middle, high and, deep convective clouds is estimated from the respective total number of cloud layers. Hence one should not compare the percentage occurrences of different clouds during different seasons with the absolute values of relative humidity for different seasons. Over Shouxian (32.56° N, 116.78° E) location, Zhang et al. (2010) reported that the percentage occurrence of low-, middle-, high-level clouds and deep convective clouds is 20.1%, 19.3%, 59.5%, and 1.1%, respectively.**

- 215  
216  
217  
218  
219  
220
9. Why figure 14 is discussed in summary section? Almost all the results presented in the study or below 12.5 km and the radiative effects shown in figure 14 are peaking near tropopause. There is no sufficient discussion on how single and multi-layered clouds will affect the radiative process. Authors have to discuss this aspect in details or remove this figure and corresponding discussion.

**Reply: Our main objective is to estimate the radiative forcing due to different cloud layers. In the current manuscript we restrict to detection of different cloud layers and their effect on temperature structure. In the follow-up manuscript we deal with radiative forcing. These aspects are also clearly mentioned in the manuscript. (Line 597 - 599)**

- 225  
226  
227  
228  
229  
230
10. There is a scope for improving the English grammar and the writing style. One gets the feeling that there are more statistics than the science in this manuscript. I suggest the authors to spend time on providing brief scientific explanations to their observations.

**Reply: We have considered the reviewer suggestion and improved the English of the manuscript and also included scientific explanation of the results. However, in the current manuscript we restrict our analysis to detection of different cloud**

layers and present their statistics during different seasons. In the follow-up manuscript we will deal with radiative forcing due to different cloud layers. These aspects are also clearly mentioned in the manuscript.

**Minor comments:**

Line 248: Background weather condition should be replaced by background meteoroidal conditions. The term ‘weather’ should be used to address the refers to shorter period variations

**Reply: Corrected. (Line 264, 265, 278)**

Line 340: Solar heating is diabatic process not adiabatic

**Reply: Corrected. (Line 357)**

**We once again thank the reviewer for providing detailed comments/suggestions for betterment of the manuscript.**

**---END---**

### Replies to Reviewer #3 Comments/suggestions

The paper documents the cloud vertical distribution over a tropical Indian station, Gadanki using the long-term radiosonde measurements. The authors classify the clouds based on the occurrence altitude and discuss their variations for different season. Investigating the cloud vertical profile is an interesting research topic due to their role in earth's radiation budget and difficulty in parameterizations of clouds in models. One of my main concern is the cloud height estimation, which is not been compared with any other measurements and lack of discussion on the observed cloud structure with large-scale environments. The manuscript is publishable, but needs careful consideration of the points listed below.

**Reply: First of all we wish to thank the reviewer for going through the manuscript carefully, appreciating actual content of the manuscript and providing constructive comments/suggestions which made us to improve the manuscript content further.**

1. The authors mentioned "Cloud Vertical Structure in all the seasons including diurnal variation over Indian region is made for the first time." Is the cloud variability observed over Gadanki can be considered as a representative over the Indian region?

**Reply: Diurnal variability in Cloud Vertical Structure of middle and upper layers in multi-layer cloud configuration over Gadanki can be considered as a representative over Indian region. However, the diurnal variability of CVS of single-layer and lower layer of multi-layer configuration might vary from location to location as it depends on topography, land use and land surface and geo-location.**

2. Ln 223: Pandit et al. (2015) studied the cirrus clouds climatology over the same station from lidar measurement. Why authors have not compared the cloud height estimated from radiosonde with lidar measurements. The aim of this task is to verify the accuracy in cloud height estimation from radiosonde. What precaution the author has taken to estimate cloud height during the raining condition, especially during monsoon?

**Reply: Kindly note that Pandit et al. (2015) used only lidar measurements to investigate cirrus clouds. This lidar can provide measurements between 8 and 30 km only (Mie channel) and we will not get any information below this altitude. However, in the present study, Cloud Vertical Structure is examined only upto 12.5 km altitude as the accuracy in RH measurements is poor at higher altitudes. Note that LIDAR gives the vertical structure of the cirrus clouds (occur at higher altitude). Also, LIDAR is operated mostly during cloud free conditions (cirrus cloud and clear sky conditions). Further, the timings of Radiosonde and LIDAR measurements are different. Hence we did not do inter comparison study with LIDAR observations.**

**In general we will not release the balloon during moderate to heavy rain conditions. However, we have done visual inspection of each radiosonde profile. RH profiles which show continuous saturation with height were discarded. These aspects are mentioned in the revised manuscript.**

3. Ln 227: How many cases do you have CPS measurement with radiosonde? What threshold of cloud number concentration the authors consider to define cloud layer from

CPS measurement? The number concentration is higher between 10 and 15 km not for the lower altitude.

**Reply:** We have only two cases of simultaneous measurements of Radiosonde and CPS Sonde from Gadanki location. Hence, the comparison of cloud number concentration and CVS structure is qualitative. We have not put any threshold on cloud particle concentration. Yes, we agree with the reviewer that the cloud particle number concentration is higher in top layer (10 – 16 km) but not for lower layers. This could be due to relatively smaller thickness of lower layers. We may need more number of simultaneous observations for further study.

4. Ln 240: homogeneous cloudiness..... How the authors defined it.

**Reply:** Homogeneous cloudiness mean that nearly uniform OLR values occurred for more than 50 km radius around Gadanki location.

5. For Fig.4, please mention the latitude and longitudinal average the authors have considered.

**Reply:** Figure 4c describe the monthly mean OLR at Gadanki location (KALPANA OLR grid location is 79.125° E, 13.375° N). We have also estimated monthly mean OLR values 0.25° around this grid point and could see results do not change. Please see enclosed Supplementary Figure S1 for this clarification.

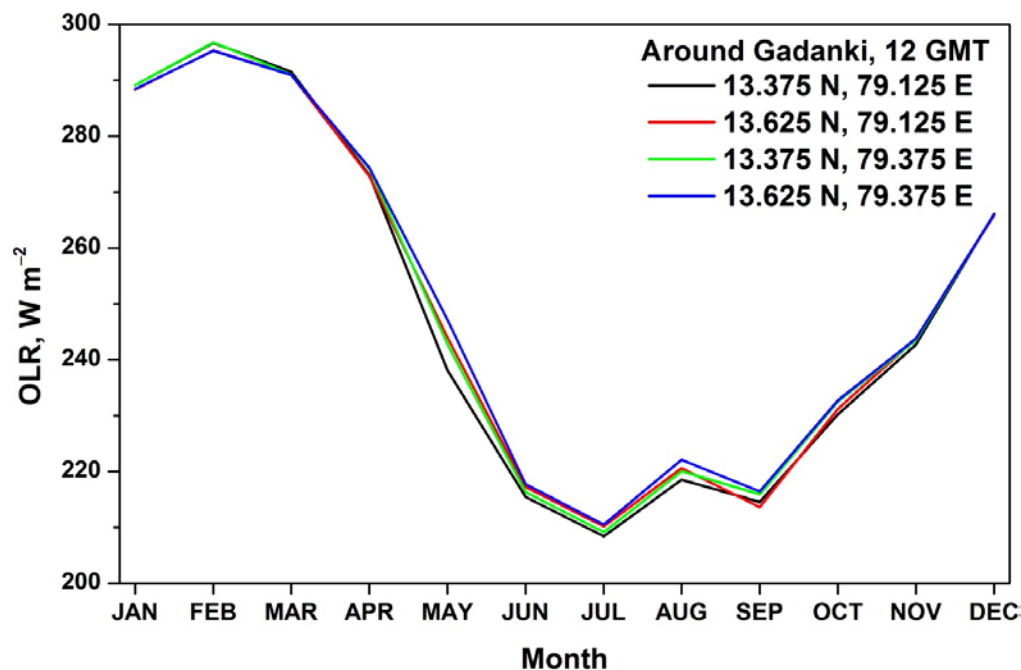


**Figure S1.** Monthly mean Outgoing Longwave Radiation (OLR) around Gadanki obtained using KALPANA-1 data during Apr. 2006 to May 2017.

6. Ln283: Change to ‘between 12 and 15 km’



333 | **Reply: Done. (Line 301)**

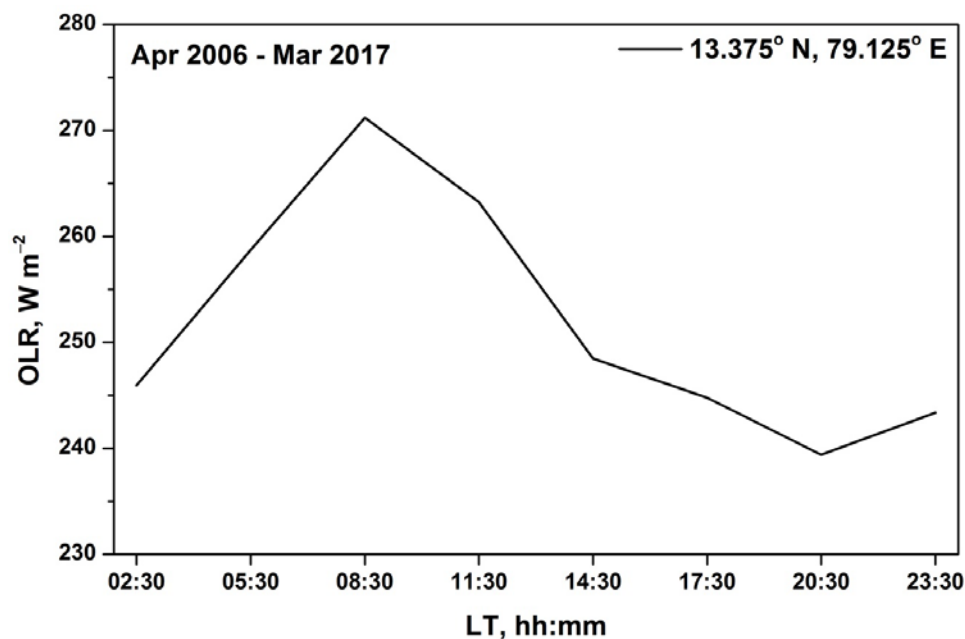
- 334
- 335 7. Ln 311: Fig 5: Diurnal variability of cloud is difficult to understand as variability of one-,
- 336 two-, three- and more-layer clouds are different. What could be the possible reason to
- 337 have maximum occurrence of cloud during mid-night to early morning. Also bit
- 338 surprising to see afternoon occurrence of cloud is less. Authors considered OLR as a
- 339 proxy for convection. It will be interesting to see the OLR diurnal variation also.

340 **Reply: As suggested by reviewer we have shown the diurnal variability in OLR at**

341 **Gadanki location in supplementary Figure S2. From the Figure S2 it is evident that**

342 **OLR values shows low values from evening to early morning hours with minimum**

343 **OLR value at 20:30 LT.**



344 **Figure S2.**Diurnal variations in Outgoing Longwave Radiation (OLR) over Gadanki obtained

345 using KALPANA-1 data during Apr. 2006 to May 2017.

- 346
- 347
- 348 8. Ln 371: Fig. 8c, the cloud thickness is up to 12 km for all season (even though the
- 349 occurrence percentage is less). Under what thermodynamic conditions such tall clouds
- 350 develop over the measurement site? Why such thick clouds are absent in fig 6 and fig. 7.

351 **Reply: In general, the factors which trigger the deep convection are strong surface**

352 **heating, moisture availability at the surface and mid troposphere, and some lifting**

353 **mechanism to lift the surface parcel above the level of free convection. Over the**

354 **Gadanki location, the different lifting mechanisms are: strong wind shear because of**

355 **low level jet during monsoon season; strong buoyancy force due to relatively higher**

356 **surface temperature during pre-monsoon period; orographic lifting as this location**

357 **is surrounded by hills.**

358 **Figure 8c is the cloud thickness observed over Gadanki location with long-term**

359 **(11 years) radiosonde data at 17:30 LT. Whereas Figure 6 and 7 are diurnal**

variations in one-layer and two-layer clouds obtained using Tropical Tropopause Dynamics (TTD) campaigns data (2010-2014). During these campaigns, the radiosondes were launched every three hourly for continuous three days in each month during Dec. 2010 to Mar. 2014. Hence deep convective clouds are not seen in Figure 6 and Figure 7.

9. Ln 412: 'The outflow caused by the deep convective systems could be responsible . . .'  
Do authors have any analysis to support their argument?

**Reply:** In general, after the dissipation of deep convective clouds they spread large anvils and remain persist as high level clouds for longer duration. These high level clouds could be due to in-situ generated Convective Systems or else propagated from the surrounding Oceans. Especially during monsoon season, deep convective clouds embedded in northward propagating convective systems originated over Indian Ocean and westward/northwestward propagating convective systems over the Bay of Bengal, dissipate over Indian land region (e.g. Sikka and Gadgil, 1980; Lawrence and Webster, 2002; Goswami, 2005; Jiang et al., 2011) and they contribute majorly to the high level cloud occurrence. In general, the high level clouds follow background winds at those levels. Due to the strong westerly winds in the upper levels, high level clouds which are originated from MCS over Bay of Bengal advect into the Indian land region and contribute to the high level cloud occurrence. Some of these aspects are included in the revised manuscript. (Line 430- 438)

10. Ln 467: 'This could be due to interactions between the different layers of cloud'. What kind of interaction, authors want to infer? Please demonstrate.

**Reply:** Interaction we mean here is longwave radiative effects. We have made the following correction. (Line 491- 495)

“ This could be due to the exchange of longwave radiation between cloud base of upper layer and cloud top of lower layer. As a result, the strong reduction in longwave radiation cooling at the top of the lower layer of cloud in the presence of upper layers of cloud (Zhang et al., 2010; Wang et al., 1999; Chen and Cotton, 1987).”

11. Ln 502: Please mention the climatological onset date of monsoon over Gadanki. What criteria authors considered to define onset of monsoon.

**Reply:** Arrival date over Gadanki is picked up manually from the yearly onset date lines over India map given by IMD. The mean arrival of southwest monsoon date for the period of analysis is on 7 June with  $\pm 4$  days.

We once again thank the reviewer for providing detailed comments/suggestions for betterment of the manuscript.

---END---

## Cloud vertical structure over a tropical station obtained using long-term high resolution Radiosonde measurements

Nelli Narendra Reddy, MadineniVenkatRatnam\*, GhouseBasha and VarahaRavikiran

National Atmospheric Research Laboratory, Department of Space, Gadanki-517112, India.

\*vratnam@narl.gov.in

### Abstract

Cloud vertical structure, including top and base altitudes, thickness of cloud layers, and the vertical distribution of multi-layer clouds affects the large-scale atmosphere circulation by altering gradients in the total diabatic heating/cooling and latent heat release. In this study, long-term (11 years) observations of high vertical resolution radiosondes are used to obtain the cloud vertical structure over a tropical station, Gadanki (13.5° N, 79.2° E), India. The detected cloud layers are verified with independent observations using cloud particle sensor (CPS) sonde launched from the same station. High-level clouds account for 69.05%, 58.49%, 55.5%, and 58.6% of all clouds during pre-monsoon, monsoon, post-monsoon, and winter seasons, respectively. The average cloud base (cloud top) altitude for low-level, middle-level, high-level and deep convective clouds are 1.74 km (3.16 km), 3.59 km (5.55 km), 8.79 km (10.49 km), and 1.22 km (11.45 km), respectively. Single-layer, two-layer, and three-layer clouds account for 40.80%, 30.71%, and 19.68% of all cloud configurations, respectively. Multi-layer clouds occurred more frequently during the monsoon with 34.58%. Maximum cloud top altitude and the cloud thickness occurred during monsoon season for single-layer clouds and the uppermost layer of multiple layer cloud configurations. In multi-layer cloud configurations, diurnal variations in the thickness of upper layer clouds are larger than those of lower layer clouds. Heating/cooling in the troposphere and lower stratosphere due to these clouds layers is also investigated and found peak cooling (peak warming) below (above) the Cold Point Tropopause (CPT) altitude. The magnitude of cooling (warming)

increases from single-layer to four or more-layer cloud occurrence. Further, the vertical structure of clouds is also studied with respect to the arrival date of Indian summer monsoon over Gadanki.

**Keywords:** Cloud vertical structure, Single-layer clouds, Multi-layer clouds, Cloud base, top and thickness

## 1. Introduction

Clouds are vital in driving the climate system as they play important role in radiation budget, general circulation and hydrological cycle (Ramanathan et al., 1989; Rossow and Lacis, 1990; Wielicki et al., 1995; Li et al., 1995; Stephens, 2005; Yanget al., 2010; Huang, 2013). By interacting with both shortwave and long-wave radiation, clouds play crucial role in the radiative budget at the surface, within and at the top of the atmosphere (Li et al., 2011; Ravi Kiran et al., 2015; George et al., 2018). Clouds and the general circulation of Earth's atmosphere are linked in an intimate feedback loop. Clouds result from the water vapor transports and cooling by atmospheric motions. The forcing for the atmospheric circulation is significantly modified by vertical and horizontal gradients in the radiative and latent heat fluxes induced by the clouds (Chahine et al., 2006 and Li et al., 2005). The complexity of the processes involved, the vast amount of information needed, including vertical and spatial distribution, and the uncertainty associated with the available data, all add difficulties to determine how clouds contribute to climate change (e.g., Heintzenberg and Charlson, 2009). In particular, knowledge about cloud type is very important, because the overall impact of clouds on the Earth's energy budget is difficult to estimate, as it involves two opposite effects depending on cloud type (Naud et al., 2003). Low, highly reflective clouds tend to cool the surface, whereas high, semi-transparent clouds tend to warm it, because they let much of the shortwave radiation through but are opaque to the long-wave

radiation. Whereas deep convective clouds (DCCs) neither warm nor cool the surface, because their cloud greenhouse and albedo forcing's nearly balance. However, DCCs produce fast vertical transport, redistributing water vapor and chemical constituents and influence the thermal structure of the Upper Troposphere and Lower Stratosphere (UTLS) (Biondi et al., 2012).

Changes in the cloud vertical structure (locations of cloud top and base, number and thickness of cloud layers) affect the atmospheric circulations by modifying the distribution of radiative and latent heating rates within the atmosphere (e.g., Slingo and Slingo, 1988; Randall et al., 1989; Slingo and Slingo, 1991; Wang and Rossow, 1998; Li et al., 2005 and Chahine et al., 2006; Cesana and Chepfer, 2012; Rossow and Zhang, 2010; Rossow et al., 2005; Wang et al., 2014b). The effects of cloud vertical structure (CVS) on atmospheric circulation have been described using atmospheric models by many authors. Crewell et al. (2004) underlined the importance of clouds in multiple scattering and absorption of sunlight, processes that have a significant impact on the diabatic heating in the atmosphere. The vertical gradients in the cloud distribution were somewhat more important to the circulation strength than horizontal gradients (Rind and Rossow, 1984). These complex phenomena are not yet fully understood and are subject to large uncertainties. In fact, the assumed or computed vertical structure of cloud occurrence in general circulation models (GCMs) is one of the main reasons why different models predict a wide range of future climates. For example, most GCMs underestimate the cloud cover, while only a few overestimate it (Xi et al., 2010). Therefore, to improve the understanding of cloud-related processes, and then to increase the predictive capabilities of large-scale models (including global circulation models), better and more accurate observations of CVSs are needed. The present work is a contribution towards addressing this need.

Formatted: Font color: Blue

476 | Ground-based instruments (e.g. Warren et al., 1988; Hahn et al., 2001), active sensor  
477 | satellites (e.g. Stephens et al., 2008; Winker et al., 2007) and upper air measurements  
478 | from radiosondes (Wang et al., 2000) are usually applied to observe and describe the CVS.  
479 | Ground-based instruments such as lidar, cloud radar and ceilometers provide cloud  
480 | measurements with continuous temporal coverage; Lidars and ceilometers are very efficient  
481 | at detecting clouds and can locate the bottom of cloud layer precisely, but cannot usually  
482 | detect the cloud top, due to attenuation of the beam within the cloud. The vertically pointing  
483 | cloud radar is able to detect the cloud top, although signal artifacts can cause difficulties  
484 | during precipitation (Nowak et al., 2008). On the other hand, passive sensor satellite data,  
485 | such as from ISCCP (the International Satellite Cloud Climatology Project) and MODIS (the  
486 | Moderate Resolution Imaging Spectroradiometer), do exist limitations. For example, the thin  
487 | clouds are indistinguishable from aerosols in ISCCP when optical thickness is less than 0.3–  
488 | 0.5) (Rossow and Garder, 1993); Both ISCCP and MODIS underestimate low-level clouds  
489 | and overestimate middle-level cloud (Li et al., 2006; Naud and Chen, 2010). Hence,  
490 | conventional passive-sensor satellite measurmentsdata, largely miss the comprehensive  
491 | information on the vertical distribution of cloud layers. The precipitation radar and TRMM  
492 | Microwave Imager on-board the Tropical Rainfall Measuring Mission (TRMM) satellite are  
493 | helpless in observing small-size particles despite of its capability of penetrating rainy cloud  
494 | and obtaining the internal three-dimensional information, and only larger rainfall particles  
495 | can be observed due to limitations of its working broadband. On the other hand, active  
496 | sensors such as the Cloud Profiling Radar (CPR) on CloudSat and the Cloud-Aerosol Lidar  
497 | with Orthogonal Polarization (CALIOP) aboard CALIPSO (Cloud Aerosol Lidar and Infrared  
498 | Pathfinder Satellite Observation) satellites are achieving notable results by including a  
499 | vertical dimension to traditional satellite images. CPR is a 94GHz nadir-looking radar which  
500 | is able to penetrate the optically thick clouds, while CALIOP is able to detect tenuous cloud

Formatted: Indent: First line: 1.27  
cm

layer that are below the detection threshold of radar. In other words, it has the ability to detect shallow clouds. Therefore, accurate location of cloud top and complete vertical structure information of cloud can be obtained by the combined use of CPR and CALIOP, because of their unique complementary skills. Previous researches have shown that CloudSat/CALIPSO data are credible compared with ISCCP and ground observation data (Sassen and Wang, 2008; Naud and Chen, 2010; Kim et al., 2011; Noh et al., 2011; Jiang et al., 2011). However, because the repeat time of these polar orbiting satellites for any particular location is very large, the time resolution of such observations is low (L'Ecuyer and Jiang, 2010; Qian et al., 2012). Both ground-based and space-based measurements have the problem of overlapping cloud layers that hide each other.

For completeness here we listed other techniques which have been developed for detecting cloud top heights from passive sensors. The CO<sub>2</sub>-slicing method uses CO<sub>2</sub> differential absorption in the thermal infrared spectral range (Rossow and Schiffer, 1991; King et al., 1992; Platnick et al., 2003). Ultraviolet radiances can also be used as rotational Raman scattering causes depletion or filling of solar Fraunhofer lines in the UV spectrum, depending on the Rayleigh scattering above the cloud (Joiner and Bhartia, 1995; de Beek et al., 2001). Similarly, the polarization of reflected light, at visible shorter wavelength, due to Rayleigh scattering carries information on cloud top height (Goloub et al., 1994; Knibbe et al., 2000). Finally, cloud top height can also be retrieved by applying geometrical methods to stereo observations (Moroney et al., 2002; Seiz et al., 2007; Wu et al., 2009). Global Navigation Satellite System (GNSS) Radio Occultation (RO) profiles were used to detect the convective cloud top heights (Biondi et al., 2013). Recently, Biondi et al. (2017) used GNSS RO profiles to detect the top altitude of volcanic clouds and analyzed their impact on thermal structure of ~~UTL~~Upper Troposphere and Lower Stratosphere. Multi-angle and bi-spectral measurements in the O<sub>2</sub> A-band were used to derive the cloud top altitude and cloud

Formatted: Indent: First line: 0.63 cm

geometrical thickness (Merlin et al., 2016 and references therein). However, this method is restricted to homogeneous plane-parallel clouds. For heterogeneous clouds or when aerosols lay above the clouds the spectra of reflected sunlight in the O<sub>2</sub> A-band will get modified.

An indirect way to perform estimations of CVS is by using atmospheric thermodynamic profiles as measured by radiosondes. Radiosondes can penetrate atmospheric (and cloud) layers to provide in situ data. The profiles of temperature, relative humidity and pressure measured by radiosondes provide information about the CVS by identifying saturated levels in the atmosphere (Zhang et al., 2010). In fact, radiosonde measurements were probably the best measurements for obtaining the CVS from the ground (Wang et al., 2000; Eresmaa et al., 2006; Zhang et al., 2010). Very recently, George et al. (2018) provided CVS over India during depression (D) and non-depression (ND) events during South West monsoon season (July 2016) using one month of campaign data. However, detailed CVS in all the seasons including diurnal variation over Indian region is not made so far to the best of our knowledge.

Our main objective is to examine the temperature structure of UTLS region during the occurrence of single-layer and multi-layer clouds over Gadanki location (13.5° N, 79.2° E). In the first, we focus to report the CVS using long-term (11 years) high vertical resolution radiosonde observations. The paper is organized as follows: data and methodology are described in section 2. In section 3, background weather conditions during the period of analysis are described. Results and discussion are given in section 4. Finally, the summary and major conclusion drawn from the present study is provided in section 5.

## **2. Data and Methodology**

### **2.1. Data**

In this study, long-term (11 years) observations of high vertical resolution radiosonde (Vaisala RS-80, RS-92; Meisei RS-01GII, RS-6G, RS-11G, IMS-100) data is used to analyze CVS over a tropical station, Gadanki. There is no significant change in the accuracies



of the meteorological parameters from these different radiosonde makes. Most of these radiosondes were launched around 1730 Local Time, LT (LT=UT+0530 h). In general we will not release the balloon during moderate to heavy rain conditions. However, we have done visual inspection of each radiosonde profile. RH profiles which shows continuous saturation with height were discarded. Figure 1 shows the monthly percentage of radiosonde data available during Apr. 2006 to May 2017. Total 3313 launches were made, out of which 98.9% and 86.6% reached altitudes greater than 12.5 km and 20 km, respectively. The data which have balloon burst altitude less than 12.5 km (1.1%) are discarded. Also, we have put condition that the number of profiles in a month should be more than seven to represent that month. After applying these two conditions the total number of profiles came to 3251. In addition, to study the diurnal variations in CVS over Gadanki, we made use of radiosonde observations taken from Tropical Tropopause Dynamics (TTD) campaigns (VenkatRatnam et al., 2014b) conducted during Climate and Weather of Sun Earth Systems (CAWSES) India Phase II program (Pallamraju et al., 2014). During these campaigns, the radiosondes were launched every three hourly for continuous three days 72-hour in each month during Dec. 2010 to Mar. 2014 except in Dec. 2012, Jan., Feb., Apr., 2013.

## 2.2. Methodology

There are several methods available in the literature to determine the CVS from the profiles of radiosonde data (Poore et al., 1995; Wang and Rossow, 1995; Chernykh and Eskridge, 1996; Minnis et al., 2005; Zhang et al., 2010). Poore et al. (1995) estimated the cloud base and cloud top using temperature-dependent dew-point depression thresholds. First, the dew-point depression must be calculated at every radiosonde level. According to Poore et al. (1995), a given atmospheric level has a cloud if  $\Delta T_d < 1.7^\circ\text{C}$  at  $T > 0^\circ\text{C}$ ,  $\Delta T_d < 3.4^\circ\text{C}$  at  $0 > T > -20^\circ\text{C}$ ,  $\Delta T_d < 5.2^\circ\text{C}$  at  $T < -20^\circ\text{C}$ .

575 Wang and Rossow (1995) used the temperature, pressure and RH profiles and computed RH  
 576 with respect to ice instead of liquid water for levels with temperatures lower than 0 °C. To this  
 577 new RH profile they have applied two RH thresholds (min RH = 84% and max RH = 87%). In  
 578 addition, if RH at the base (top) of the moist layer is lower than 84%, a RH jump exceeding  
 579 3% must exist from the underlying (above) level. According to the Chernykh and Eskridge  
 580 (1996) method, the necessary condition for the existence of clouds in a given atmospheric  
 581 level is that the second derivatives with respect to height ( $z$ ) of temperature and RH to be  
 582 positive and negative, respectively, i.e.,  $T''(z) \geq 0$  and  $RH''(z) \leq 0$ . Minnis et al. (2005)  
 583 provided an empirical parameterization that calculates the probability of occurrence of a  
 584 cloud layer using RH and air temperature from radiosondes. First, RH values must be  
 585 converted to RH with respect to ice when temperature is less than -20 °C; on the other hand,  
 586 the profile has to be interpolated every 25 hPa up to the height of 100 hPa. An expression to  
 587 estimate the cloud probability ( $P_{cld}$ ) as a function of temperature and RH is then applied; in  
 588 this formula, where RH is given the maximum influence as it is the most important factor in  
 589 cloud formation. Finally, a cloud layer is set wherever  $P_{cld} \geq 67\%$ . The Zhang et al. (2010)  
 590 method is an improvement on the Wang and Rossow (1995) method. Instead of a single RH  
 591 threshold, Zhang et al. (2010) applied altitude-dependent thresholds without the requirement  
 592 of the 3% RH jump at the cloud base and top.

593 Costa-Sueros et al. (2014) compared the CVS derived from these five methods described  
 594 above by using 193 radiosonde profiles acquired at the Atmospheric Radiation Measurement  
 595 (ARM) Southern Great Plains site during all seasons of the year 2009. The performance of  
 596 the five methods has been assessed by comparing with Active Remote Sensing of Clouds  
 597 (ARSCL) data taken as a reference. Costa-Sueros et al. (2014) concluded that three of the  
 598 methods (Poore et al., 1995; Wang and Rossow, 1995; and Zhang et al., 2010) perform  
 599 reasonably well, giving perfect agreements for 50% of the cases and approximate agreements

for 30% of the cases. The other methods gave poorer results (lower perfect and/or approximate agreement, and higher false positive, false negative or not coincident detections). Among the three methods, Zhang et al. (2010) method is the most recent version of the treatment initially proposed in Poore et al. (1995) and Wang and Rossow (1995), and provides good enough results (a perfect agreement of 53.9% and an approximate agreement of 29.5%). Thus, the algorithm of Zhang et al. (2010) is used for detecting cloud layers in our analysis and we provide details of Zhang et al. (2010) algorithm.

Cloud layers are associated with high RH values above some threshold as the radiosonde penetrates through them. Cloud detection algorithm of Zhang et al. (2010) employs three height-resolving RH thresholds to determine cloud layers: minimum and maximum RH thresholds in cloud layers (min-RH and max-RH), and minimum RH thresholds within the distance of two contiguous layers (inter-RH). The height-resolving thresholds of max-RH, min-RH, and inter-RH values are specified in Table 1. The algorithm begins by converting RH with respect to liquid water to RH with respect to ice at temperatures below 0° C (see example in Figure 2). The accuracy of RH measurement is less than 5% up to the altitude 12.5 km and hence the RH profile is examined from the surface to the 12.5 km (~ 200 hPa) altitude to find cloud layers in seven steps: (1) the base of the lowest moist layer is determined as the level when RH exceeds the min-RH corresponding to this level; (2) above the base of the moist layer, contiguous levels with RH over the corresponding min-RH are treated as the same layer; (3) the top of the moist layer is identified when RH decreases to that below the corresponding min-RH or RH is over the corresponding min-RH but the top of the profile is reached; (4) moist layers with bases lower than 500 m AGL (Above Ground Level) and thickness less than 400 m are discarded; (5) the moist layer is classified as a cloud layer if the maximum RH within this layer is greater than the corresponding max-RH at the base of this moist layer; (6) two contiguous layers are considered as a one-layer cloud if the

distance between these two layers is less than 300 m or the minimum RH within this distance is more than the maximum inter-RH value within this distance; and (7) clouds are discarded if their thicknesses are less than 100 m.

At measurement location, we have Boundary Layer Lidar and Mie Lidar. When there is occurrence of multi-layer configuration, BLL does not give accurate cloud base altitude for higher layers. Whereas, Mie LIDAR gives the vertical structure of the cirrus clouds (usually occur at higher altitude). In the pPresent study, CVSloud Vertical Structure is examined only upto 12.5 km altitude as the accuracy in RH measurements is poor at higher altitudes. Also, Mie LIDAR is operated mostly during cloud free conditions (only during cirrus cloud or clear sky conditions). Further, the timings of Radiosonde and LIDAR measurements are different. Hence, we did not do inter comparison study with ground based LIDAR observations. On the other hand, CLOUDSAT/CALIPSO overpasses over experiment location are around 02 LT and 14 LT. Whereas regular radiosonde launches are around 1730 LT. Hence, we did not do inter comparison study between regular radiosonde and CLOUDSAT/CALIPSO measurements. However, we have three hourly radiosonde observations for continuous three days in every month during Tropical Tropopause Dynamics (TTD) campaigns. Unfortunately, we did not get collocated (space and time) measurements from CLOUDSAT/CALIPSO and Radiosonde during these campaigns.

Formatted: List Paragraph

Before proceeding further, it is desired to verify the identified layers of clouds are correct or not with independent observations. For that we have launched Cloud Particle Sensor (CPS) sonde (Fujiwara et al., 2016) at Gadanki, which provides profile of cloud number concentration. Results from a flight of RS-11G radiosonde and Cloud Particle Sensor (CPS) Sonde on the same balloon launched at 02 LT on 04 Aug. 2017 at Gadanki, India is shown in

Figure 2. Sudden increase in the cloud number concentration within the detected cloud layers indicates the cloud layer boundaries detected in the present study are accurate.

The drawback of using the radiosonde data for detecting the CVS at a given location is the radiosonde horizontal displacement, due to the drift produced by the wind. However, irrespective of the season, the maximum horizontal drift of radiosonde when it reaches the 12.5 km altitude is always less than 20 km (VenkatRatnam et al., 2014a). One may expect different background features within this 20 km particularly the localised convection that may influence the CVS. In order to assess this aspect, we used outgoing longwave radiation (OLR) as a proxy for tropical convection. Figure 3(a-d) describes the seasonal mean distribution of OLR (from KALPANA-1 satellite) around Gadanki location obtained during pre-monsoon, monsoon, post-monsoon and, winter seasons averaged during 2006 – 2017. It can be noted that irrespective of the season, homogeneous cloudiness prevailed for more than 50 km radius around Gadanki location. Hence the CVS detected from the radiosonde can be treated as representative of Gadanki location.

Methodology described in section 2.2 to detect CVS is applied on high vertical resolution radiosonde data acquired during Apr. 2006 to May 2017 from Gadanki, as well as special radiosondes launches during TTD campaigns from Oct. 2010 to Apr. 2014. Results are presented in Section 4. Before going further, it is desirable to examine the background ~~meteorological weather~~ conditions prevailing over Gadanki during different seasons.

### 3. Background ~~meteorological weather~~ conditions

National Atmospheric Research Laboratory (NARL) at Gadanki is located about 120km northwest of Chennai (Madras) on the east coast of the southern Indian peninsula. This station is surrounded by hills with a maximum altitude of 350–400m above the station, and the station is at an altitude of 375ma.m.s.l. (hereinafter all altitudes are mentioned above mean sea level only). The local topography is complex with a number of small hillocks

around and a high hill of ~1km about 30km from the balloon launching site in the northeast direction. The detailed topography of Gadanki is shown in Basha and Ratnam (2009). Gadanki receives 53% of the annual rainfall during the southwest monsoon (Jun. to Sep.) and 33% of the annual rainfall during the northeast monsoon (Oct. to Dec.) (Rao et al., 2008a). The rainfall during the southwest monsoon occurs predominantly during the evening to midnight period. About 66% of total rainfall is convective in nature, while the remaining rain is widespread stratiform in character (Rao et al., 2008a).

Background meteorological conditions prevailing over the observational site are briefly described based on the radiosonde data collected during Apr. 2006 to May 2017. The seasons are classified as winter (December-January- February), pre-monsoon (March-April-May), monsoon (June-July-August-September), post-monsoon (October-November). The climatological monthly mean contours of the temperature anomalies, relative humidity, zonal and meridional winds are shown in Figure 4(a-d), respectively. From surface to 1 km altitude, temperature anomalies show seasonal variability with warmer temperatures during pre-monsoon months and relatively cooler temperatures during winter season (Figure 4a). Temperature anomalies do not show significant variations seasonally from 1 km altitude to the middle troposphere, but shows variations in the lower stratosphere. There exist significant seasonal variations in the RH (Figure 4b). During winter, RH is small (40 – 50%) from surface to ~ 3 km altitude and is almost negligible above. However, during the other seasons, particularly in the peak monsoon months (Jul. and Aug.), large RH values (60–70%) are noticed up to 10 km altitude.

During winter, easterlies exist up to 4–6 km altitude and westerlies above (Figure 4c). There seem to be weak easterlies above the altitude of 14km during the pre-monsoon. During the monsoon season low level westerlies exist below 7–8km and easterlies above. The Tropical Easterly Jet (TEJ) is prevalent over this region in the SW monsoon season, with

peak velocity sometimes reaching more than  $40\text{ms}^{-1}$  (Roja Raman et al., 2009). There exist large vertical shears during monsoon in the zonal wind. Easterlies exist up to 20 km altitude during post-monsoon season. In general, meridional velocities are very small and are northerlies up to 8 km and southerlies above in all the seasons, except during monsoon (Figure 4d). During the winter and monsoon, relatively stronger southerlies and northerlies prevailed, respectively, between 12 to 15 km altitudes. A clear annual oscillation can be noticed in both zonal and meridional velocities. Similar variations are also observed by the MST radar located at the same site in between 4 and 20 km (Ratnam et al., 2008; Basha and Ratnam, 2009; Debashis Nath et al., 2009). Monthly mean OLR around Gadanki at 1730 LT is shown in Figure 4e. Low values of OLR ( $< 220 \text{ W m}^{-2}$ ) around Gadanki location indicate that the occurrence of very deep convection during the monsoon season, consistent with the occurrence of high RH values up to 10 km altitude during monsoon season (Figure 4b).

#### 4. Results

By adopting the methodology described in section 2.2 we have detected a total of 4309 Cloud layers from 3251 radiosonde launches at Gadanki location during the period of data analysis. For each season, cloud layers during Apr. 2006 – May 2017 are averaged to obtain the composite picture of CVS. Seasonal variability in cloud layers is discussed in section 4.2.

##### 4.1. Diurnal variation of single-layer and multi-layer clouds

There are studies on the diurnal variation of cloud layers outside the Indian region. For example, over Porto Santo Island during the Atlantic Stratocumulus Transition Experiment (ASTEX) by Wang et al. (1999), over San Nicolas Island during First ISCCP Regional Experiment (FIRE) by Blaskovic et al. (1990), Over Shouxian ( $32.56^\circ \text{ N}$ ,  $116.78^\circ \text{ E}$ ) location by Zhang et al. (2010). As per authors knowledge there are no studies on diurnal variability of cloud layers over Indian region. For the first time, over Indian land region, the diurnal variability of cloud layers are studied by using radiosonde observations taken from TTD

campaigns. Figure 5(a-d) describes the diurnal variations of single-layer and multi-layer clouds during pre-monsoon, monsoon, post-monsoon, and winter seasons over Gadanki region. As mentioned in section 2.1, from Dec. 2010 to Mar.2014, we have launched radiosondes every three hourly for continuous three days in every month except during Dec. 2012, Jan., Feb., Apr., 2013. The total number of profiles taken during pre-monsoon, monsoon, post-monsoon, and winter seasons are 160, 254, 101, and 199, respectively. Among these the number of cloudy profiles are 93 in pre-monsoon, 241 in monsoon, 63 in post-monsoon, and 96 in winter seasons.

From the Figure 5(a-d), for four seasons, diurnal variations of cloud occurrence show a maximum between 23 to 05 LT and a minimum at 14 LT, except during monsoon season. During monsoon season which, a minimum in cloud occurrence occurred at 11 LT. Using Infrared Brightness temperature data over Indian region Gambheer and Bhat (2001), Zuidema (2003), Reddy and Rao (2018) observed the maximum frequency of occurrence of clouds during late night early morning hours. Percentage occurrence of one-layer and multi-layer clouds shows noticeable diurnal variations in all seasons except in monsoon season. Maximum percentage occurrence in one-layer clouds is at 08 LT in pre-monsoon season and it is at 17 LT during post-monsoon and winter seasons. For all the seasons, the maximum percentage occurrence in multi-layer clouds is between 20 to 05 LT. Figure 6(a-d) describes the mean vertical locations (base and top) and cloud thicknesses of one-layer clouds during pre-monsoon, monsoon, post-monsoon, and winter seasons, respectively. During monsoon season, the maximum in cloud top altitude is at 05 LT and minimum is at 14 LT (Figure 6(b)). In general, cloud base of one-layer cloud occur at higher altitude between 11 – 14 LT and it occur relatively low altitudes between 20 – 08 LT. Except during post-monsoon season, the single-layer clouds are high-level clouds with base is greater than 5 km most of the times. During post-monsoon season, the single-layer clouds are low-level at 05 LT



(cloud-base altitude of 1.4 km) and middle level-clouds between 14 – 02 LT (Figure 6c). During pre-monsoon and monsoon seasons, thickness of single-layer clouds reaching a maximum at 23 LT and a minimum at 14 LT (Figure 6(a-b)). The minimum in one-layer cloud thickness at 14 LT is due to the increase of cloud base altitude and simultaneous decrease of cloud top altitude. There is not much variability in thickness of one-layer clouds during post-monsoon and winter seasons (Figure 6(c-d)). Figure 7(a-d) and Figure S1(a-d) are same as Figure 6(a-d) but for two-layer and three-layer clouds. Similar to one-layer cloud, the cloud base of bottom-layer of two-layer clouds show maximum between 11 – 14 LT and minimum between 20 – 08 LT. Thickness of top layer and bottom layer of two-layer clouds reaching a minimum value between 11 – 14 LT. Upper layer of two-layer clouds show a maximum in thickness at 23 LT and minimum at 11 LT during monsoon season (Figure 7(b)).

The cloud maintenance and development are strongly modulated by [adiabatic processes](#), namely solar heating and longwave (LW) radiative cooling (Zhang et al., 2010). Near noontime (11 - 14 LT), solar heating is so strong that (1) evaporation of cloud drops may occur and (2) atmospheric stability may increase thus suppressing cloud development. So near noontime, the vertical development of single-layer clouds and the vertical development of the uppermost layer of multiple layers of cloud are suppressed due to solar heating. This effect is predominant during monsoon season for one-layer and two-layer clouds (Figures 6(b) and 7(b)), during pre-monsoon and post-monsoon seasons for three-layer clouds (Figures S1a and S1c). However, for lower layers of cloud in a multiple-layer cloud configuration, solar heating is greatly reduced because of the absorption and scattering processes of the upper layers of cloud. In general maximum in surface temperature occurs around 15:20 LT (Reddy and Rao, 2018). The ground surface is warmer than any cloud layer so through the exchange of LW radiation, the cloud base gains more energy. This facilitates cloud

development and leads to a maximum in cloud altitude and thickness between 14 – 17 LT (Figures 7a, 7b, 7d and S1a). This effect is predominant during winter season for two layer clouds (Figure 7d) and during pre-monsoon season for three-layer clouds (Figure S1a). As the sun sets, LW radiative cooling starts to dominate over shortwave (SW) radiative warming. Cloud top temperatures begin to lower, which increases atmospheric instability and fuels the development of single-layer clouds and the uppermost layer of cloud in multiple-layer cloud configurations. At sunset, solar heating diminishes and LW cooling strengthens, which may explain why there is a peak between 20 – 23 LT in the thickness of one-layer clouds and the uppermost layer of two-layercloud. This effect is clearlyobserved in the monsoon season (Figures 6b, 7b, S1b). We conclude that diurnal variability in base, top and thickness for single-layer, two-layer and, three-layer clouds are significant. Hence there can be a bias in cloud vertical structure when we are studying the composite over a season by using polar satellites.

Next section, we show the seasonal variability in cloud layers using long-term (11 years) observations of high vertical resolution radiosonde overGadanki. Note that most of these radiosondes were launched around 1730 LT hence there will be bias in the results due to diurnal variability of cloud layers which we have discussed above. Hence the results related to seasonal variability of cloud layers are only representative of 1730 LT.

#### **4.2. Seasonal variability in the cloud layers**

Figure 8(a-c) describes the percentage occurrence of base, top and thickness of cloud layersobserved during different seasons over Gadanki. The cloud base altitude shows a bimodal distribution in all seasons except during pre-monsoon season (Figure 8a). During pre-monsoon season, the peak of cloud base altitude distribution is observed at ~6.2 km (~7.5%). During other three seasons (monsoon, post-monsoon and winter), the first peak in cloud base altitude is observed between 2 and 3 km altitude region and the second peak is

observed at ~6.2 km. Using CLOUDSAT observations over the Indian monsoon region, Das et al. (2017) also reported that the cloud base altitude over Indian monsoon region shows a bimodal distribution. However, the first peak in cloud base altitude is observed at ~14 km while the second maximum is at 2 km.

The cloud top altitude increases above 12 km altitude and have a maximum at 12.5 km in all seasons (Figure 8b). Note that we restrict maximum altitude as 12.5 km due to limitation in providing reliable water vapour above that altitude from normal radiosondes. At lower altitudes, during the monsoon season the peak in cloud top altitude is at 2.9 km and it increases to 3.3 km during the post-monsoon season. However we have also checked the cloud vertical structure till 18 km. There is no significant difference in the cloud base and cloud top altitude distribution (See Figure S2). Das et al. (2017) reported that there are two peaks in the cloud top altitude; one at ~17 km and other is at ~3 km. The peaks in cloud base and cloud top at higher altitudes as observed by Das et al. (2017) could be due to the occurrence of cirrus clouds.

The cloud base altitude values are subtracted from the cloud top altitude for each cloud layer to extract the cloud thickness. Figure 8(c) describes the percentage occurrence of the cloud thickness observed during different seasons. The occurrence of thicker clouds decreases exponentially. The cloud thickness has a maximum below 500 m for all seasons, which constituted about 34.7%, 26.5%, 31.2% and 36.6% of the total observed cloud layers during pre-monsoon, monsoon, post-monsoon and winter seasons, respectively. In general, for all seasons, more than 65% of clouds layers have cloud thickness < 2 km.

Different cloud types occurring at different height regions have a spectrum of effects on the radiation budget (Behrangi et al., 2012). Therefore, the clouds have been classified into four groups based on the cloud base altitude and their thickness (Lazarus et al., 2000 and Zhang et al., 2010): (1) low-level clouds with bases lower than 2 km and thickness less than 6

Formatted: Font color: Auto

824 km; (2) middle-level clouds with bases ranging from 2 to 5 km; (3) high-level clouds with  
 825 bases greater than 5 km; and (4) deep convective cloud (hereafter called DCC) with bases less  
 826 than 2 km and thicknesses greater than 6 km. These four types of clouds account for 11.97%,  
 827 26.71%, 59.36% and 1.95% of all cloudy cases, respectively. Figure 9(a-d) describe the mean  
 828 vertical locations (base and top), cloud thicknesses and percentage occurrence of low-,  
 829 middle-, high-level clouds, and DCC observed during different seasons. At Gadanki location,  
 830 there is a distinct persistence of the high-level clouds over all the seasons. The occurrence of  
 831 the high-level clouds is 69.05%, 58.49%, 55.5%, 58.6% during the pre-monsoon, monsoon,  
 832 post-monsoon, and winter seasons, respectively (Figure 9c). In general, after the dissipation  
 833 of deep convective clouds they spread large anvils and remain persist as high level  
 834 clouds for longer duration. These high level clouds could be due to in-situ generated  
 835 Convective Systems or else propagated from the surrounding Oceans. Zuidema (2003)  
 836 reported that the deep convective systems generated over central and west Bay of Bengal  
 837 (BoB) advect toward the inland region of southern peninsular India and dissipates. In general,  
 838 the high level clouds follow background winds at those levels. Especially during  
 839 monsoon season, due to the strong westerly winds in the upper levels, high level clouds  
 840 which are originated from MCS over BoB advect into the Indian land  
 841 region and contribute to the high level cloud occurrence. Hence Zuidema (2003) reported  
 842 that the deep convective systems generated over central and west BoB advect toward the  
 843 inland region of southern peninsular India and dissipates. The outflow caused by the deep  
 844 convective systems could be responsible for the higher percentage occurrence of high-level  
 845 clouds. The low-level (middle-level) clouds contribute about 3.74%, 10.45%, 16.27%, and  
 846 20.89% (27.04%, 29.35%, 24.28%, and 18.67%) of all cloudy cases during the pre-monsoon,  
 847 monsoon, post-monsoon, and winter seasons, respectively (Figure 9a-b).

Thickesses of low-, middle-, high-level clouds have minimum values during winterseason and maximum values in monsoon season (Figure 9a-c). Whereas DCChave minimum thickness in winter and maximum in pre-monsoon season (Figure 9d). The average cloud base (cloud top) altitudes for low-, middle-, high-level clouds and deep convective clouds are 1.74 km (3.16 km), 3.59 km (5.55 km), 8.79 km (10.49 km), and 1.22 km (11.45 km), respectively.Over Indian summer monsoon region, Das et al. (2017) reported that the percentage occurrence of high-level clouds is more than the other three cloud types. Over Shouxian (32.56° N, 116.78° E) location, Zhang et al. (2010) reported that the percentage occurrence of low-, middle-, high-level clouds and deep convective clouds is 20.1%, 19.3%, 59.5%, and 1.1%, respectively.

#### 4.2.1. Single-layer and Multi-layer clouds

By interacting with both shortwave and longwave radiation, clouds play crucial role in the radiative budget at the surface, within and at the top of the atmosphere.Over the tropics, the zonal mean net cloud radiative effect differences between multi-layer clouds and single-layer clouds were positive and dominated by the shortwave cloud radiative effect differences (Li et al., 2011). This is because, the multi-layer clouds reflect less sunlight to the top of the atmosphere and transmit more to the surface and within the atmosphere than the single-layer clouds as a whole. As a result, multi-layer clouds warm the earth-atmosphere system when compared to single-layer clouds(Li et al., 2011). In this study, we studied the occurrence of single-layer and multi-layer clouds obtained during different seasons at Gadanki location. The percentage occurrence of single-layer, two-layer, three-layer and four- or more- layer clouds during pre-monsoon, monsoon, post-monsoon and winter seasons are shown in Figure 10(a-d). Single-layer, two-layer and three-layer clouds account for 40.80%, 30.71%, and 19.68% of all cloud configurations, respectively. Even though the low frequency of occurrence of one-layer clouds over Gadanki, they exhibit pronounced seasonal variation in

magnitude with very low frequency during pre-monsoon season. This may be due to the strong warm and dry atmospheric conditions from surface to boundary layer top (Figure 4a and 4b). Percentage occurrence of single-layer (multi-layer) clouds during pre-monsoon, monsoon, post-monsoon and winter seasons are 7.7%, 14.2%, 8.48% and 10.42% (7.93%, 34.58%, 10.83% and 5.86%), respectively. There is a significant occurrence of multi-layer clouds during monsoon season than other seasons indicating that the development of multi-layer clouds is favorable under warm and moist atmospheric conditions (Figures 4a and 4b). Among the different cloud layers, the two-layer clouds have maximum percentage occurrence (16.6%) during monsoon season (Figure 10b). Luo et al. (2009) reported the occurrence of multi-layer clouds over the Indian region during the summer season and attributed it to the complex cloud structure associated with the monsoon system. Zhang et al. (2010) reported that multi-layer cloud occurrence frequency is relatively higher during summer months (Jun., Jul. and Aug.) than autumn months (Sep., Oct. and Nov.) over Shouxian. Recently, Using the four years of combined observations of Cloudsat and CALIPSO, Subrahmanyam and Kumar (2017) reported the maximum frequency of occurrence of two-layer clouds over Indian sub-continent during Jun. Jul. and Aug months. This they attributed to the presence of Indian summer monsoon circulation over this region, which is dominated by the formation of various kinds of clouds such as cumulus, stratocumulus, cirrus etc. Very recently, George et al. (2018) reported CVS using the radiosonde launches during depression (D) and non-depression (ND) events in South West monsoon season using one month of field campaign data over Kanpur, India.

Figure 11(a-c) describe the mean vertical locations (base and top) and cloud thicknesses of single-layer, two-layer and three-layer clouds during different seasons. Except during winter season, single-layer clouds are thicker than the layers forming multi-layer clouds. Also, upper layer clouds are thicker than lower layer clouds in multi-layer clouds. This could

Formatted: Font: 12 pt, Not Bold

~~be due to the exchange of longwave radiation between cloud base of upper layer and cloud top of lower layer. As a result, the strong reduction in longwave radiation cooling at the top of the lower layer of cloud in the presence of upper layers of cloud (Zhang et al., 2010; Wang et al., 1999; Chen and Cotton, 1987). This could be due to interactions between the different layers of cloud. This feature might also be associated with the strong reduction in longwave radiation cooling at the top of the lower layer of cloud in the presence of upper layers of cloud (Zhang et al., 2010; Wang et al., 1999; Chen and Cotton, 1987).~~

Irrespective of the season, single-layer clouds are high-level clouds i.e cloud base is > 5 km (Figure 11a). Maximum cloud top altitude and the cloud thickness occurred during monsoon season for single-layer clouds (Figure 11a) and the uppermost layer of multi-layer cloud configurations (Figure 11b-c). This is consistent with the low OLR values ( $< 220 \text{ W m}^{-2}$ ) observed during monsoon season (Figure 11d). Except during pre-monsoon season, cloud base, cloud top and cloud thickness values of lower layer of multi-layer clouds are same during monsoon, post-monsoon and winter seasons. Whereas during pre-monsoon season, cloud base and cloud top of lower layer of multi-layer clouds occurred at relatively higher altitudes (Figure 11b-c). Similarly, there are no significant variations in cloud thickness in middle layer of three-layer clouds between the seasons. However, cloud base and cloud top of middle layer of three-layer clouds during pre-monsoon season occurred relatively at higher altitudes than the other three seasons (Figure 11c). Table 2 describes the mean base, top and thicknesses of cloud layers of single-layer, two-layer and three-layer clouds. In the two-layer clouds, the thickness of the upper level cloud layer is about the same as those of single-layer clouds. In the three-layer clouds, the base and top heights of the lowest layer of cloud are similar to those of the lowest layer of cloud in two-layer clouds.

#### 4.3. Variability in CVS with respect to SW monsoon arrival over Gadanki

CVS play an important role in the summer monsoon because they can significantly affect the atmospheric heat balance through latent heating caused by water phase changes and through scattering of radiation. In this section we discuss the variability in different clouds with respect to the date of arrival of southwest (SW) monsoon over Gadanki. SW monsoon onset occurs over Kerala coast (south west coast of India) during the last week of the May or first week of June. In general, the climatological mean monsoon onset over Kerala (MOK) is on 1 June with  $\pm 7$  days. It is to be noted that the climatology onset date is obtained from IMD long term onset dates and arrival date over Gadanki is picked up manually from the yearly onset date lines over India map given by IMD.

Figure 12 shows the composite (2006 – 2016) percentage occurrence of clear sky and cloud days (Figure 12a), low-level, middle-level, high-level and deep convective clouds (Figure 12b), and one-, two-, three- and four or more- layer clouds (Figure 12c) with respect to monsoon arrival date. Figures 13(a-c) describe the mean vertical locations (base and top) and cloud thicknesses of single-layer, two-layer clouds with respect to monsoon arrival date. Day zero in Figures 12(a-b) and Figures 13(a-b) indicates the date of monsoon arrival over Gadanki location. The percentages occurrences of clear sky conditions prior to the monsoon arrival over Gadanki location decreases and reduce to zero on the date of monsoon arrival (Figure 12a). This indicates the estimated dates of monsoon arrival over Gadanki location are correct. From day four onwards the cloudiness start increases and peaks on day 18 (Figure 12a). The percentage occurrence of middle level clouds decreases till 5 days prior to the monsoon arrival (Figure 12b). Subsequently middle level clouds percentage increases and does not show significant variability later to the monsoon arrival. There are no deep convective clouds prior and during the monsoon arrival over Gadanki location (Figure 12b). They occurred on day 3, 9, 10, 17 and 20. During and later to the arrival of the monsoon, the



percentage occurrence of multilayer clouds is always greater than the single layer clouds except day three and four (Figure 12c). Day zero it is noted that single layer clouds are high level clouds and they are thicker with thickness  $\sim 6.7$  km(Figure 13a). In two layer clouds the bottom layer is middle layer cloud and top layer is high level cloud(Figure 13b). The bottom layer is thicker than the top layer.During deep convective clouds and middle level, single layer clouds prevailed. The thickness of single layer clouds show large variability with thickness ranging from 300 m to 5 km during the first week later to the arrival of the monsoon. In the second week, the thickness ranges from 2 km to 5 km(Figure 13a).Later to the arrival of the monsoon, thickness of bottom layer in two layer cloud is relatively higher than the top layer (Figure 13b). Thicker single layer clouds and bottom layer of two layer clouds later to the monsoon arrival over Gadanki is due to the increase of tropospheric water vapor.

## 5. Summary

Cloud vertical structure (CVS) is studied for the first time over India by using long-term high vertical resolution radiosonde measurements at Gadanki location obtained during Apr. 2006 to May 2017. In order to obtain diurnal variation in CVS, we have used 3 hourly launched radiosondes for 3 days 72 hours in each month during Dec. 2010 to Mar. 2014. CVS is obtained following Zhang et al. (2010) where it relay on height-resolved relative humidity thresholds. After obtaining the cloud layers they are segregated to low, middle and high level clouds depending upon their altitude of occurrence. Detected layers are verified using independent measurements from cloud particle sensor (CPS) sonde launched from same location. Very good match between these two independent measurements is noticed.

First,the diurnal variations in CVS over Gadanki is studied using radiosonde observations taken from TTD campaigns conducted during CAWSES India Phase II program.During pre-monsoon and monsoon seasons, thickness of single-layer clouds reaches a maximum at 23

971 LT and a minimum at 14 LT. Upper layer of two-layer clouds show a maximum in thickness  
972 at 23 LT and minimum at 11 LT during monsoon season. Radiosonde measurements around  
973 1730 LT were used to study the seasonal variability in CVS. After ascertaining the cloud  
974 layers they are segregated into different season to obtain the season variation of CVS. High-  
975 level clouds account for 69.05%, 58.49%, 55.5%, and 58.6% of cloud layers identified during  
976 pre-monsoon, monsoon, post-monsoon, and winter seasons, respectively, indicating high  
977 cloud layers being most prevalent at Gadanki location. Single-layer, two-layer, and three-layer  
978 clouds account for 40.80%, 30.71%, and 19.68% of all cloud configurations, respectively.  
979 Multi-layer clouds occurred more frequently during the monsoon with 34.58%. Maximum  
980 cloud top altitude and the cloud thickness occurred during monsoon season for single-layer  
981 clouds and the uppermost layer of multi-layer cloud configurations.

982 Further, we have discussed the variability in different clouds with respect to the date of  
983 arrival of southwest (SW) monsoon over Gadanki location. Prior, during and later to the SW  
984 monsoon arrival over Gadanki location, high level clouds occurrence is more than the other  
985 cloud types. Whereas the middle level cloud occurrence decreases till 5 days prior to the  
986 monsoon arrival and increases subsequently. There are no deep convective clouds prior and  
987 during the monsoon arrival over Gadanki location. The thickness of single layer clouds shows  
988 large variability during the first week later to the arrival of the monsoon. But it increases  
989 significantly between 8 – 11 days later to the monsoon arrival. Later to the arrival of the  
990 monsoon, thickness of bottom layer in two layer cloud is relatively higher than the top layer.  
991 Thicker single layer clouds and bottom layer of two layer clouds later to the monsoon arrival  
992 over Gadanki is due to the increase of tropospheric water vapor.

993 These cloud layers are expected to affect significantly to the background temperature  
994 in the troposphere and lower stratosphere. The composite (2006-2016) temperature profiles  
995 during clear sky, one-layer, two-layer, three-layer and four or more-layer cloud occurrences

are shown in Figure 14. The temperature differences between the cloudy (single-, two-, three-, four or more- layer) and clear sky conditions are shown with dash lines in Figure 14. The striking result here is that occurrence of peak cooling (peak warming) below (above) the Cold Point Tropopause (CPT) altitude. The magnitude of cooling (warming) increases from single-layer to four or more-layer cloud occurrence. The peak cooling and warming during four or more-layer cloud occurrence are 0.9 K (at 15.7 km) and 3.6 K (at 18.1 K). Both single-layer and multi-layer clouds show warming between 5 km and 14.5 km altitude region. The peak warming of 0.8 K at 9.5 km for single-layer cloud, and 1.3 K at 10.2 K for multi-layer clouds are observed and these altitudes are close to the cloud top altitude of single layer cloud and top layer of multi-layer clouds (Table 2). The detailed study on the impact of single-layer and multi-layer clouds on ~~upper troposphere and lower stratosphere~~ (UTLS) dynamics and thermodynamics structure will be investigated in our subsequent article including their radiative forcing.

## Acknowledgements

We are grateful to the National Atmospheric Research Laboratory (NARL), Gadanki, for providing necessary data for the present study.

## References

- Basha, G., Ratnam, M.V.: Moisture variability over Indian monsoon regions observed using high resolution radiosonde measurements. Atmos. Res. 132–133, 35–45. doi:10.1016/j.atmosres.2013.04.004, 2013.
- Basha, G., Ratnam, M.V.: Identification of atmospheric boundary layer height over a tropical station using high-resolution radiosonde refractivity profiles: Comparison with GPS radio occultation measurements. J. Geophys. Res. Atmos. 114, D16101. doi:10.1029/2008JD011692, 2009.
- Behrangi, A., Kubar, T., Lambriksen, B.: Phenomenological Description of Tropical Clouds

1021 Using CloudSat Cloud Classification. Mon. Weather Rev. 140, 3235–3249.  
 1022 doi:10.1175/MWR-D-11-00247.1, 2012.

1023 Biondi, R., Randel, W. J., Ho, S.-P., Neubert, T. and Syndergaard, S.: Thermal structure of  
 1024 intense convective clouds derived from GPS radio occultations, Atmos. Chem. Phys., 12(12),  
 1025 5309–5318, doi:10.5194/acp-12-5309-2012, 2012.

1026 Biondi, R., Ho, S.-P., Randel, W.J., Neubert, T., Syndergaard, S.: Tropical cyclone cloud-top  
 1027 height and vertical temperature structure detection using GPS radio occultation  
 1028 measurements. J. Geophys. Res. Atmos. 118, 5247–5259. doi:10.1002/jgrd.50448, 2013.

1029 Biondi, R., Steiner, A. K., Kirchengast, G., Brenot, H. and Rieckh, T.: Supporting the  
 1030 detection and monitoring of volcanic clouds: A promising new application of Global  
 1031 Navigation Satellite System radio occultation, Adv. Sp. Res., 60(12), 2707–2722, doi:  
 1032 10.1016/j.asr.2017.06.039, 2017.

1033 Blaskovic, M., Davies, R., Snider, J.B.: Diurnal Variation of Marine Stratocumulus over San  
 1034 Nicolas Island during July 1987. Mon. Weather Rev. 119, 1469–1478. doi:10.1175/1520-  
 1035 0493(1991)119<1469:DVOMSO>2.0.CO;2, 1990.

1036 Cesana, G., Chepfer, H.: How well do climate models simulate cloud vertical structure? A  
 1037 comparison between CALIPSO-GOCCP satellite observations and CMIP5 models. Geophys.  
 1038 Res. Lett. 39, n/a-n/a. doi:10.1029/2012GL053153, 2012.

1039 Chahine, M.T., Pagano, T.S., Aumann, H.H., Atlas, R., Barnett, C., Blaisdell, J., Chen, L.,  
 1040 Divakarla, M., Fetzer, E.J., Goldberg, M., Gautier, C., Granger, S., Hannon, S., Irion, F.W.,  
 1041 Kakar, R., Kalnay, E., Lambrechts, B.H., Lee, S.-Y., Le Marshall, J., McMillan, W.W.,  
 1042 McMillin, L., Olsen, E.T., Revercomb, H., Rosenkranz, P., Smith, W.L., Staelin, D., Strow,  
 1043 L.L., Susskind, J., Tobin, D., Wolf, W., Zhou, L.: AIRS: Improving Weather Forecasting and  
 1044 Providing New Data on Greenhouse Gases. Bull. Am. Meteorol. Soc. 87, 911–926.

**Formatted:** Font: (Default) +Body  
(Times New Roman)

doi:10.1175/BAMS-87-7-911, 2006.

Chen, C., Cotton, W.R.: The Physics of the Marine Stratocumulus-Capped Mixed Layer. *J. Atmos. Sci.* 44, 2951–2977. doi:10.1175/1520-0469(1987)044<2951:TPOTMS>2.0.CO;2, 1987.

Chernykh, I. V, Eskridge, R.E.: Determination of Cloud Amount and Level from Radiosonde Soundings. *J. Appl. Meteorol.* 35, 1362–1369. doi:10.1175/1520-0450(1996)035<1362:DOCAAL>2.0.CO;2, 1996.

Costa-Surós, M., Calbó, J., González, J.A., Long, C.N.: Comparing the cloud vertical structure derived from several methods based on radiosonde profiles and ground-based remote sensing measurements. *Atmos. Meas. Tech.* 7, 2757–2773. doi:10.5194/amt-7-2757-2014, 2014.

Crewell, S., Bloemink, H., Feijt, A., García, S.G., Jolivet, D., Krasnov, O.A., Van Lammeren, A., Löhnert, U., Van Meijgaard, E., Meywerk, J., Quante, M., Pfeilsticker, K., Schmidt, S., Scholl, T., Simmer, C., Schröder, M., Trautmann, T., Venema, V., Wendisch, M., Willén, U.: THE BALTEX BRIDGE CAMPAIGN: An Integrated Approach for a Better Understanding of Clouds. *Bull. Am. Meteorol. Soc.* 85, 1565–1584. doi:10.1175/BAMS-85-10-1565, 2004.

Das, S.K., Golhait, R.B., Uma, K.N.: Clouds vertical properties over the Northern Hemisphere monsoon regions from CloudSat-CALIPSO measurements. *Atmos. Res.* 183, 73–83. doi:https://doi.org/10.1016/j.atmosres.2016.08.011, 2017.

de Beek, R., Vountas, M., Rozanov, V. V., Richter, a., and Burrows, J. P.: The ring effect in the cloudy atmosphere, *Geophys. Res. Lett.*, 28, 721–724, doi:10.1029/2000GL012240, 2001.

Eresmaa, N., Karppinen, A., Joffre, S.M., Räsänen, J., Talvitie, H.: Mixing height determination by ceilometer. *Atmos. Chem. Phys.* 6, 1485–1493. doi:10.5194/acp-6-1485-2006, 2006.

Fujiwara, M., Sugidachi, T., Arai, T., Shimizu, K., Hayashi, M., Noma, Y., Kawagita, H.,

1070 Sagara, K., Nakagawa, T., Okumura, S., Inai, Y., Shibata, T., Iwasaki, S., Shimizu, A.;  
 1071 Development of a cloud particle sensor for radiosonde sounding. *Atmos. Meas. Tech.* 9,  
 1072 5911–5931. doi:10.5194/amt-9-5911-2016, 2016.

1073 Gambheer, A. V, Bhat, G.S.: Diurnal variation of deep cloud systems over the Indian region  
 1074 using INSAT-1B pixel data. *Meteorol. Atmos. Phys.* 78, 215–225. doi:10.1007/s703-001-  
 1075 8175-4, 2001.

1076 George, G., Sarangi, C., Tripathi, S. N., Chakraborty, T., & Turner, A.: Vertical structure and  
 1077 radiative forcing of monsoon clouds over Kanpur during the 2016 INCOMPASS field  
 1078 campaign. *J. Geophys. Res.*, 123. <https://doi.org/10.1002/2017JD027759>, 2018.

1079 Goloub, P., Deuze, J. L., Herman, M., and Fouquart, Y.: Analysis of the  
 1080 POLDER polarization measurements performed over cloud covers, *IEEE T. Geosci. Remote*,  
 1081 32, 78–88, doi:10.1109/36.285191, 1994.

1082 Hahn, C.J., Rossow, W.B., Warren, S.G.: ISCCP Cloud Properties Associated with Standard  
 1083 Cloud Types Identified in Individual Surface Observations. *J. Clim.* 14, 11–28.  
 1084 doi:10.1175/1520-0442(2001)014<0011:ICPAWS>2.0.CO;2, 2001.

1085 Heintzenberg, J., Charlson, R.J. (Eds.): Clouds in the perturbed climate system: their  
 1086 relationship to energy balance, atmospheric dynamics and precipitation. MIT Press,  
 1087 Cambridge, UK, 2009.

1088 Huang, Y.: On the Longwave Climate Feedbacks. *J. Clim.* 26, 7603–7610. doi:10.1175/JCLI-  
 1089 D-13-00025.1, 2013.

1090 Jiang, X., Waliser, D.E., Li, J.-L., Woods, C.: Vertical cloud structures of the boreal summer  
 1091 intraseasonal variability based on CloudSat observations and ERA-interim reanalysis. *Clim.*  
 1092 *Dyn.* 36, 2219–2232. doi:10.1007/s00382-010-0853-8, 2011.

1093 Joiner, J. and Bhartia, P. K.: The determination of cloud pressures from rotational  
 1094 Ramanscattering in satellite backscatterultraviolet measurements, *J. Geophys. Res.*, 100,  
 1095 23019–23026,doi:10.1029/95JD02675, 1995.

1096 Kim, S.-W., Chung, E.-S., Yoon, S.-C., Sohn, B.-J., Sugimoto, N.: Intercomparisons of  
 1097 cloud-top and cloud-base heights from ground-based Lidar, CloudSat and CALIPSO  
 1098 measurements. *Int. J. Remote Sens.* 32, 1179–1197. doi:10.1080/01431160903527439, 2011.

1099 Lazarus, S.M., Krueger, S.K., Mace, G.G.: A Cloud Climatology of the Southern Great Plains  
 1100 ARM CART. *J. Clim.* 13, 1762–1775. doi:10.1175/1520-  
 1101 0442(2000)013<1762:ACCOTS>2.0.CO;2, 2000.

1102 King, N. J. and Vaughan, G.: Using passive remote sensing to retrieve the vertical variationof  
 1103 cloud droplet size in marine stratocumulus: An assessment of information content and  
 1104 thepotential for improved retrievals from hyperspectral measurements, *J.Geophys. Res.*, 117,  
 1105 D15206, doi:10.1029/2012JD017896, 2012.

1106 Knibbe, W. J. J., De Haan, J. F., Hovenier, J. W., Stam, D. M., Koelemeijer, R. B. A.,  
 1107 andStammes, P.: Deriving terrestrial cloud toppressure from photopolarimetry of reflected  
 1108 light, *J. Quant. Spectrosc. Ra.*, 64, 173–199, doi:10.1016/S0022-4073(98)00135-6,2000.

1109 L’Ecuyer, T. ~S., Jiang, J. ~H.: Touring the atmosphere aboard the A-Train. *Phys. Today* 63,  
 1110 36. doi:10.1063/1.3463626, 2010.

1111 Li, J., Yi, Y., Minnis, P., Huang, J., Yan, H., Ma, Y., Wang, W., Kirk Ayers, J.: Radiative  
 1112 effect differences between multi-layered and single-layer clouds derived from CERES,  
 1113 CALIPSO, and CloudSat data. *J. Quant. Spectrosc. Radiat. Transf.* 112, 361–375.  
 1114 doi:https://doi.org/10.1016/j.jqsrt.2010.10.006, 2011.

1115 Li, Y., Liu, X., Chen, B.: Cloud type climatology over the Tibetan Plateau: A comparison of  
 1116 ISCCP and MODIS/TERRA measurements with surface observations. *Geophys. Res. Lett.*

1117 33, n/a-n/a. doi:10.1029/2006GL026890, 2006.  
 1118 Li, Z., Barker, H.W., Moreau, L.: The variable effect of clouds on atmospheric absorption of  
 1119 solar radiation. *Nature* 376, 486–490, 1995.  
 1120 Li, Z., Cribb, M.C., Chang, F.-L., Trishchenko, A., Luo, Y.: Natural variability and sampling  
 1121 errors in solar radiation measurements for model validation over the Atmospheric Radiation  
 1122 Measurement Southern Great Plains region. *J. Geophys. Res. Atmos.* 110, n/a-n/a.  
 1123 doi:10.1029/2004JD005028, 2005.  
 1124 Luo, Y., Zhang, R., Wang, H.: Comparing Occurrences and Vertical Structures of  
 1125 Hydrometeors between Eastern China and the Indian Monsoon Region Using  
 1126 CloudSat/CALIPSO Data. *J. Clim.* 22, 1052–1064. doi:10.1175/2008JCLI2606.1, 2009.  
 1127 Merlin, G., Riedi, J., Labonnote, L. C., Cornet, C., Davis, A. B., Dubuisson, P., Desmons,  
 1128 M., Ferlay, N., and Parol, F.: Cloud information content analysis of multi-angular  
 1129 measurements in the oxygen A-band: application to 3MI and MSPI, *Atmos. Meas. Tech.*, 9,  
 1130 4977-4995, doi:amt-9-4977-2016, 2016.  
 1131 Minnis, P., Yi, Y., Huang, J., Ayers, K.: Relationships between radiosonde and RUC-2  
 1132 meteorological conditions and cloud occurrence determined from ARM data. *J. Geophys.*  
 1133 *Res. Atmos.* 110, n/a-n/a. doi:10.1029/2005JD006005, 2005.  
 1134 Moroney, C., Davies, R., and Muller, J.-P.: Operational retrieval of cloud-top heights using  
 1135 MISR data, *IEEE T. Geosci. Remote*, 40, 1532–1540, doi:10.1109/TGRS.2002.801150, 2002.  
 1136 Nath, D., Venkat Ratnam, M., Jagannadha Rao, V.V.M., Krishna Murthy, B. V, Vijaya  
 1137 Bhaskara Rao, S.: Gravity wave characteristics observed over a tropical station using high-  
 1138 resolution GPS radiosonde soundings. *J. Geophys. Res. Atmos.* 114, n/a-n/a.  
 1139 doi:10.1029/2008JD011056, 2009.  
 1140 Naud, C.M., Chen, Y.-H.: Assessment of ISCCP cloudiness over the Tibetan Plateau using  
 1141 CloudSat-CALIPSO. *J. Geophys. Res. Atmos.* 115, n/a-n/a. doi:10.1029/2009JD013053,



1142 2010.

1143 Naud, C.M., Muller, J.-P., Clothiaux, E.E.: Comparison between active sensor and  
 1144 radiosonde cloud boundaries over the ARM Southern Great Plains site. *J. Geophys. Res.*  
 1145 *Atmos.* 108, n/a-n/a. doi:10.1029/2002JD002887, 2003.

1146 Noh, Y.-J., Seaman, C.J., Vonder Haar, T.H., Hudak, D.R., Rodriguez, P.: Comparisons and  
 1147 analyses of aircraft and satellite observations for wintertime mixed-phase clouds. *J. Geophys.*  
 1148 *Res. Atmos.* 116, n/a-n/a. doi:10.1029/2010JD015420, 2011.

1149 Nowak, D., Ruffieux, D., Agnew, J.L., Vuilleumier, L.: Detection of Fog and Low Cloud  
 1150 Boundaries with Ground-Based Remote Sensing Systems. *J. Atmos. Ocean. Technol.* 25,  
 1151 1357–1368. doi:10.1175/2007JTECHA950.1, 2008.

1152 Pallamraju, D., Gurubaran, S., Venkat Ratnam, M.: A brief overview on the special issue on  
 1153 CAWSES-India Phase II program. *J. Atmos. Solar-Terrestrial Phys.* 121, 141–144.  
 1154 doi:https://doi.org/10.1016/j.jastp.2014.10.013, 2014.

1155 Platnick, S., King, M. D., Ackerman, S., Menzel, W. P., Baum, B., Riedi, J. C., and Frey,  
 1156 R.: The MODIS cloud products: Algorithms and examples from Terra, *IEEE T. Geosci.*  
 1157 *Remote*, 41, 459–473, doi:10.1109/TGRS.2002.808301, 2003.

1158 Poore, K.D., Wang, J., Rossow, W.B.: Cloud Layer Thicknesses from a Combination of  
 1159 Surface and Upper-Air Observations. *J. Clim.* 8, 550–568. doi:10.1175/1520-  
 1160 0442(1995)008<0550:CLTFAC>2.0.CO;2, 1995.

1161 Qian, Y., Long, C.N., Wang, H., Comstock, J.M., McFarlane, S.A., Xie, S.: Evaluation of  
 1162 cloud fraction and its radiative effect simulated by IPCC AR4 global models against ARM  
 1163 surface observations. *Atmos. Chem. Phys.* 12, 1785–1810. doi:10.5194/acp-12-1785-2012,  
 1164 2012.

1165 Ramanathan, V., Cess, R.D., Harrison, E.F., Minnis, P., Barkstorm, B.R., Ahmad, E.,  
 1166 Hartmann, D.: Cloud-Radiative Forcing and Climate: Results from the Earth Radiation

1167 Budget Experiment. *Science* (80-. ). 243, 57 LP-63,, 1989.  
 1168 Randall, D.A.: Cloud parameterization for climate modeling: Status and prospects. *Atmos.*  
 1169 *Res.* 23, 345–361. doi:[https://doi.org/10.1016/0169-8095\(89\)90025-2](https://doi.org/10.1016/0169-8095(89)90025-2), 1989.  
 1170 Rao, T.N., Kirankumar, N.V.P., Radhakrishna, B., Rao, D.N., Nakamura, K.: Classification  
 1171 of Tropical Precipitating Systems Using Wind Profiler Spectral Moments. Part II: Statistical  
 1172 Characteristics of Rainfall Systems and Sensitivity Analysis. *J. Atmos. Ocean. Technol.* 25,  
 1173 898–908. doi:10.1175/2007JTECHA1032.1, 2008a.  
 1174 Ravi Kiran, V., Rajeevan, M., Gadhavi, H., Rao, S.V.B., Jayaraman, A.: Role of vertical  
 1175 structure of cloud microphysical properties on cloud radiative forcing over the Asian  
 1176 monsoon region. *Clim. Dyn.* 45, 3331–3345. doi:10.1007/s00382-015-2542-0, 2015.  
 1177 Reddy, N.N., Rao, K.G.: Contrasting variations in the surface layer structure between the  
 1178 convective and non-convective periods in the summer monsoon season for Bangalore  
 1179 location during PRWONAM. *J. Atmos. Solar-Terrestrial Phys.* 167, 156-168.  
 1180 doi:10.1016/j.jastp.2017.11.017, 2017, 2018.  
 1181 Rind, D., Rossow, W.B.: The Effects of Physical Processes on the Hadley Circulation. *J.*  
 1182 *Atmos. Sci.* 41, 479–507. doi:10.1175/1520-0469(1984)041<0479:TEOPPO>2.0.CO;2,  
 1183 1984.  
 1184 Roja Raman, M., Jagannadha Rao, V.V.M., Venkat Ratnam, M., Rajeevan, M., Rao, S.V.B.,  
 1185 Narayana Rao, D., Prabhakara Rao, N.: Characteristics of the Tropical Easterly Jet: Long-  
 1186 term trends and their features during active and break monsoon phases. *J. Geophys. Res.*  
 1187 *Atmos.* 114, n/a-n/a. doi:10.1029/2009JD012065, 2009.  
 1188 Rossow, W. B. and Schiffer, R. A.: ISCCP Cloud Data Products, *B. Am. Meteorol. Soc.*, 72,  
 1189 2–20, doi:10.1175/1520-0477(1991)072<0002:ICDP>2.0.CO;2, 1991.  
 1190 Rossow, W.B., Garder, L.C.: Validation of ISCCP Cloud Detections. *J. Clim.* 6, 2370–2393.  
 1191 doi:10.1175/1520-0442(1993)006<2370:VOICD>2.0.CO;2, 1993.

1192 Rossow, W.B., Lacis, A.A.: Global, Seasonal Cloud Variations from Satellite Radiance  
 1193 Measurements. Part II. Cloud Properties and Radiative Effects. *J. Clim.* 3, 1204–1253.  
 1194 doi:10.1175/1520-0442(1990)003<1204:GSCVFS>2.0.CO;2, 1990.  
 1195 Rossow, W.B., Zhang, Y.: Evaluation of a Statistical Model of Cloud Vertical Structure  
 1196 Using Combined CloudSat and CALIPSO Cloud Layer Profiles. *J. Clim.* 23, 6641–6653.  
 1197 doi:10.1175/2010JCLI3734.1, 2010.  
 1198 Rossow, W.B., Zhang, Y., Wang, J.: A Statistical Model of Cloud Vertical Structure Based  
 1199 on Reconciling Cloud Layer Amounts Inferred from Satellites and Radiosonde Humidity  
 1200 Profiles. *J. Clim.* 18, 3587–3605. doi:10.1175/JCLI3479.1, 2005.  
 1201 Sassen, K., Wang, Z.: Classifying clouds around the globe with the CloudSat radar: 1-year of  
 1202 results. *Geophys. Res. Lett.* 35, n/a–n/a. doi:10.1029/2007GL032591, 2008.  
 1203 Seiz, G., Tjemkes, S., and Watts, P.: Multiview Cloud-Top Height and Wind Retrieval with  
 1204 Photogrammetric Methods: Application to Meteosat-8 HRV Observations, *J. Appl. Meteorol.*  
 1205 *Clim.*, 46, 1182–1195, doi:10.1175/JAM2532.1, 2007.  
 1206 Slingo, A., Slingo, J.M.: The response of a general circulation model to cloud longwave  
 1207 radiative forcing. I: Introduction and initial experiments. *Q. J. R. Meteorol. Soc.* 114, 1027–  
 1208 1062. doi:10.1002/qj.49711448209, 1988.  
 1209 Slingo, J.M., Slingo, A.: The response of a general circulation model to cloud longwave  
 1210 radiative forcing. II: Further studies. *Q. J. R. Meteorol. Soc.* 117, 333–364.  
 1211 doi:10.1002/qj.49711749805, 1991.  
 1212 Stephens, G.L.: Cloud Feedbacks in the Climate System: A Critical Review. *J. Clim.* 18,  
 1213 237–273. doi:10.1175/JCLI-3243.1, 2005.  
 1214 Stephens, G.L., Vane, D.G., Tanelli, S., Im, E., Durden, S., Rokey, M., Reinke, D., Partain,  
 1215 P., Mace, G.G., Austin, R., L'Ecuyer, T., Haynes, J., Lebsock, M., Suzuki, K., Waliser, D.,  
 1216 Wu, D., Kay, J., Gettelman, A., Wang, Z., Marchand, R.: CloudSat mission: Performance and

1217 early science after the first year of operation. *J. Geophys. Res. Atmos.* 113, n/a-n/a.  
 1218 doi:10.1029/2008JD009982, 2008.  
 1219 Subrahmanyam, K.V., Kumar, K.K.: CloudSat observations of multi layered clouds across  
 1220 the globe. *Clim. Dyn.* 49, 327–341. doi:10.1007/s00382-016-3345-7, 2017.  
 1221 Uma, K.N., Kumar, K.K., Shankar Das, S., Rao, T.N., Satyanarayana, T.M.: On the Vertical  
 1222 Distribution of Mean Vertical Velocities in the Convective Regions during the Wet and Dry  
 1223 Spells of the Monsoon over Gadanki. *Mon. Weather Rev.* 140, 398–410. doi:10.1175/MWR-  
 1224 D-11-00044.1, 2012.  
 1225 Venkat Ratnam, M., Narendra Babu, A., Jagannadha Rao, V.V.M., Vijaya Bhaskar Rao, S.,  
 1226 Narayana Rao, D.: MST radar and radiosonde observations of inertia-gravity wave  
 1227 climatology over tropical stations: Source mechanisms. *J. Geophys. Res. Atmos.* 113, n/a-n/a.  
 1228 doi:10.1029/2007JD008986, 2008.  
 1229 Venkat Ratnam, M., Pravallika, N., Ravindra Babu, S., Basha, G., Pramitha, M., Krishna  
 1230 Murthy, B. V.: Assessment of GPS radiosonde descent data. *Atmos. Meas. Tech.* 7, 1011–  
 1231 1025. doi:10.5194/amt-7-1011-2014, 2014a.  
 1232 Venkat Ratnam, M., Sunilkumar, S. V, Parameswaran, K., Krishna Murthy, B. V,  
 1233 Ramkumar, G., Rajeev, K., Basha, G., Ravindra Babu, S., Muhsin, M., Kumar Mishra, M.,  
 1234 Hemanth Kumar, A., Akhil Raj, S.T., Pramitha, M.: Tropical tropopause dynamics (TTD)  
 1235 campaigns over Indian region: An overview. *J. Atmos. Solar-Terrestrial Phys.* 121, 229–239.  
 1236 doi:https://doi.org/10.1016/j.jastp.2014.05.007, 2014b.  
 1237 Wang, F., Xin, X., Wang, Z., Cheng, Y., Zhang, J., Yang, S.: Evaluation of cloud vertical  
 1238 structure simulated by recent BCC\_AGCM versions through comparison with CALIPSO-  
 1239 GOCCP data. *Adv. Atmos. Sci.* 31, 721–733. doi:10.1007/s00376-013-3099-7, 2014.  
 1240 Wang, J., Rossow, W.B.: Effects of Cloud Vertical Structure on Atmospheric Circulation in  
 1241 the GISS GCM. *J. Clim.* 11, 3010–3029. doi:10.1175/1520-

1242 0442(1998)011<3010:EOCVSO>2.0.CO;2, 1998.

1243 Wang, J., Rossow, W.B.: Determination of Cloud Vertical Structure from Upper-Air  
 1244 Observations. *J. Appl. Meteorol.* 34, 2243–2258. doi:10.1175/1520-  
 1245 0450(1995)034<2243:DOCVSF>2.0.CO;2, 1995.

1246 Wang, J., Rossow, W.B., Uttal, T., Rozendaal, M.: Variability of Cloud Vertical Structure  
 1247 during ASTEX Observed from a Combination of Rawinsonde, Radar, Ceilometer, and  
 1248 Satellite. *Mon. Weather Rev.* 127, 2484–2502. doi:10.1175/1520-  
 1249 0493(1999)127<2484:VOCVSD>2.0.CO;2, 1999.

1250 Wang, J., Rossow, W.B., Zhang, Y.: Cloud Vertical Structure and Its Variations from a 20-Yr  
 1251 Global Rawinsonde Dataset. *J. Clim.* 13, 3041–3056. doi:10.1175/1520-  
 1252 0442(2000)013<3041:CVSAIV>2.0.CO;2, 2000.

1253 Warren, S.G., Hahn, C.J., London, J., Chervin, R.M., Jenne, R.L.: Global distribution of total  
 1254 cloud cover and cloud type amounts over the ocean. doi:TN-317+STR, 212 pp, 1988.

1255 Wielicki, B.A., Harrison, E.F., Cess, R.D., King, M.D., Randall, D.A. Mission to Planet  
 1256 Earth: Role of Clouds and Radiation in Climate. *Bull. Am. Meteorol. Soc.* 76, 2125–2153.  
 1257 doi:10.1175/1520-0477(1995)076<2125:MTPERO>2.0.CO;2, 1995.

1258 Winker, D.M., Hunt, W.H., McGill, M.J.; Initial performance assessment of CALIOP.  
 1259 *Geophys. Res. Lett.* 34, n/a-n/a. doi:10.1029/2007GL030135, 2007.

1260 Wu, D. L., Ackerman, S. a., Davies, R., Diner, D. J., Garay, M. J., Kahn, B. H., Maddux, B.  
 1261 C., Moroney, C. M., Stephens, G. L., Veefkind, J. P., and Vaughan, M. A.:  
 1262 Vertical distributions and relationships of cloud occurrence frequency as observed by  
 1263 MISR, AIRS, MODIS, OMI, CALIPSO, and CloudSat, *Geophys. Res. Lett.*, 36, L09821,  
 1264 doi:10.1029/2009GL037464, 2009.

1265 Xi, B., Dong, X., Minnis, P., Khaiyer, M.M.: A 10 year climatology of cloud fraction and  
 1266 vertical distribution derived from both surface and GOES observations over the DOE ARM

1267 SPG site. J. Geophys. Res. Atmos. 115, n/a-n/a. doi:10.1029/2009JD012800, 2010.

1268 Yang, Q., Fu, Q., Hu, Y.: Radiative impacts of clouds in the tropical tropopause layer. J.

1269 Geophys. Res. Atmos. 115, n/a-n/a. doi:10.1029/2009JD012393, 2010.

1270 Zhang, J., Chen, H., Li, Z., Fan, X., Peng, L., Yu, Y., Cribb, M.: Analysis of cloud layer

1271 structure in Shouxian, China using RS92 radiosonde aided by 95 GHz cloud radar. J.

1272 Geophys. Res. Atmos. 115, n/a-n/a. doi:10.1029/2010JD014030, 2010.

1273 Zuidema, P.: Convective Clouds over the Bay of Bengal. Mon. Weather Rev. 131, 780–798.

1274 doi:10.1175/1520-0493(2003)131<0780:CCOTBO>2.0.CO;2, 2003.

1275 **Tables:**

1276

	Height-resolving RH thresholds		
Altitude range	min-RH	max-RH	inter-RH
0-2 km	92%	95%	84%
2-6 km	90%	93%	82%
6-12 km	88%	90%	78%
>12 km	75%	80%	70%

1277

1278 **Table 1.** Summary of height-resolving RH thresholds.

1279

	Multi-layer clouds	Cloud base altitude (km)	Cloud top altitude (km)	Cloud thickness (km)
	Single-layer cloud	6.32	9.24	2.92
Upper layer	two-layer clouds	8.51	11.23	2.72
	three-layer clouds	9.63	11.79	2.16
Middle layer	three-layer clouds	6.69	7.80	1.11
Lower layer	two-layer clouds	4.08	5.56	1.48
	three-layer clouds	3.04	4.31	1.27

1280

1281 | **Table 2.** Mean base, top and thicknesses of cloud layers of single-layer, two-layer and three-  
1282 layer clouds.

1283

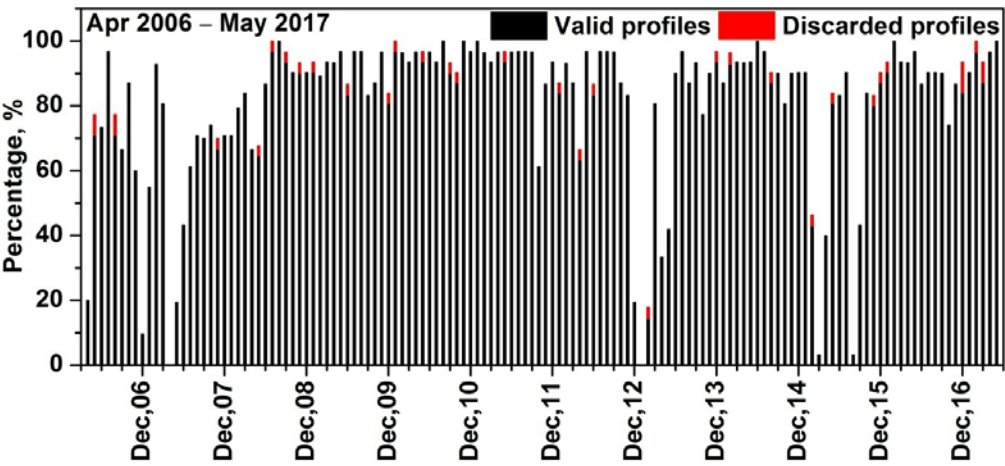
1284

1285

**Formatted:** Indent: Left: 0 cm,  
Hanging: 0.32 cm, Space Before: 0 pt,  
Line spacing: Double

1286 **Figures:**

1287



1288

1289 **Figure 1.** Monthly percentage of radiosonde data available during Apr. 2006 – May. 2017 at

1290 Gadanki. Percentage of discarded profiles in each month is also shown with red colour.

1291

Formatted: Indent: Left: 0 cm,  
Hanging: 0.32 cm



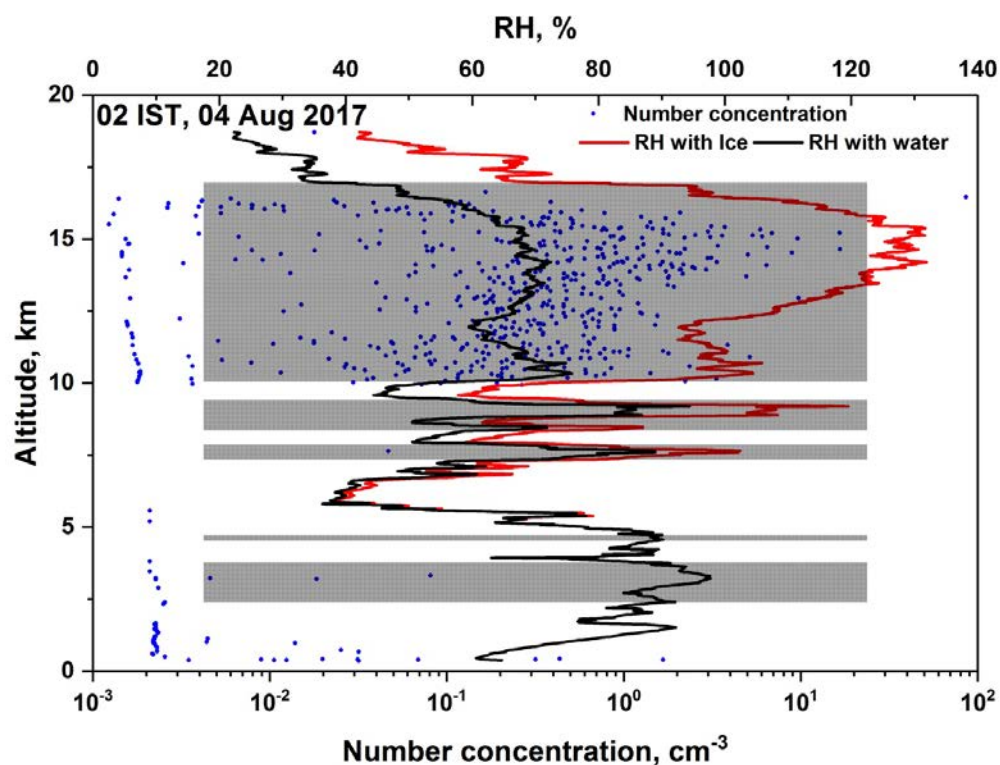


**Figure 2.** Results from a flight of RS-11G radiosonde and Cloud Particle Sensor (CPS) sonde on the same balloon launched at 02 IST on 04 Aug. 2017 at Gadanki, India. Profiles of RH estimated with respect to water (black solid line) and ice (when temperatures are less than 0°C (red solid line)), and number concentration (filled blue circles) from CPS sonde profile are shown. Detected cloud layer boundaries are shown by the filled gray rectangle boxes. Increase in the number concentration within the detected cloud layers indicates the cloud layer boundaries detected in the present study are accurate.

Formatted: Indent: Left: 0 cm, Hanging: 0.32 cm

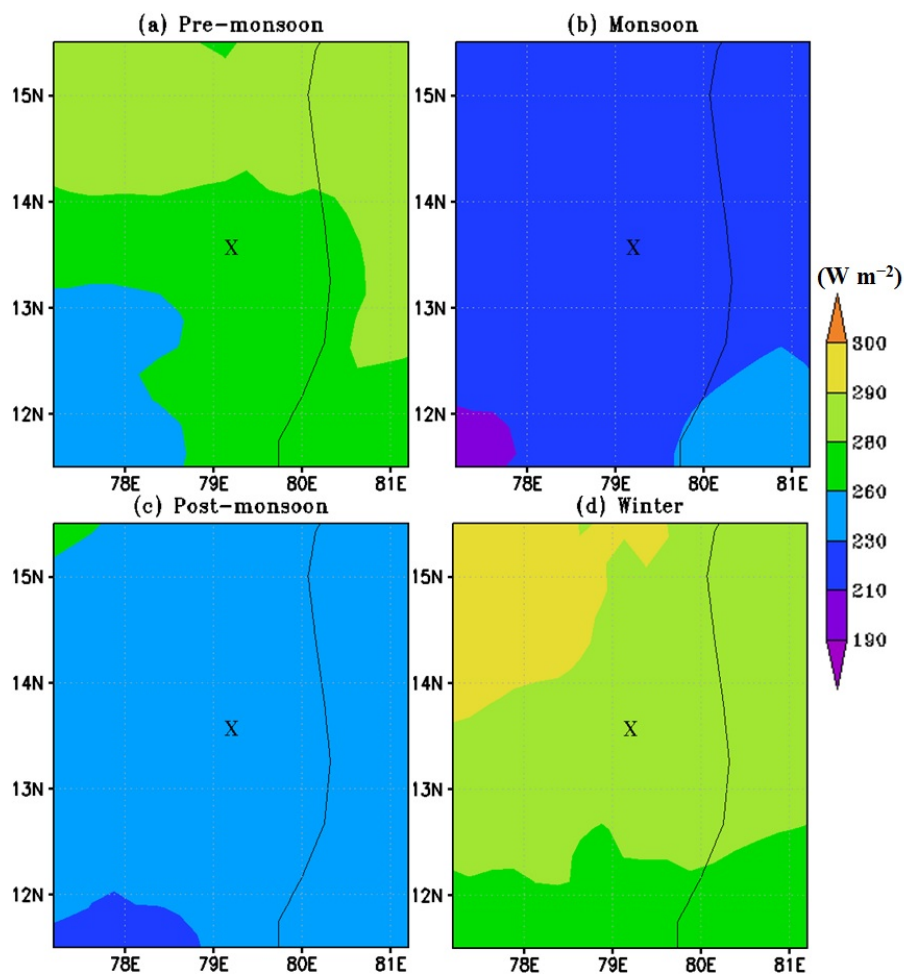


**Figure 3.** Seasonal mean distribution of OLR around Gadanki location observed during (a) Pre-monsoon, (b) Monsoon, (c) Post-monsoon and (d) Winter seasons averaged during 2006 – 2017. The symbol ‘X’ indicates the location of Gadanki.

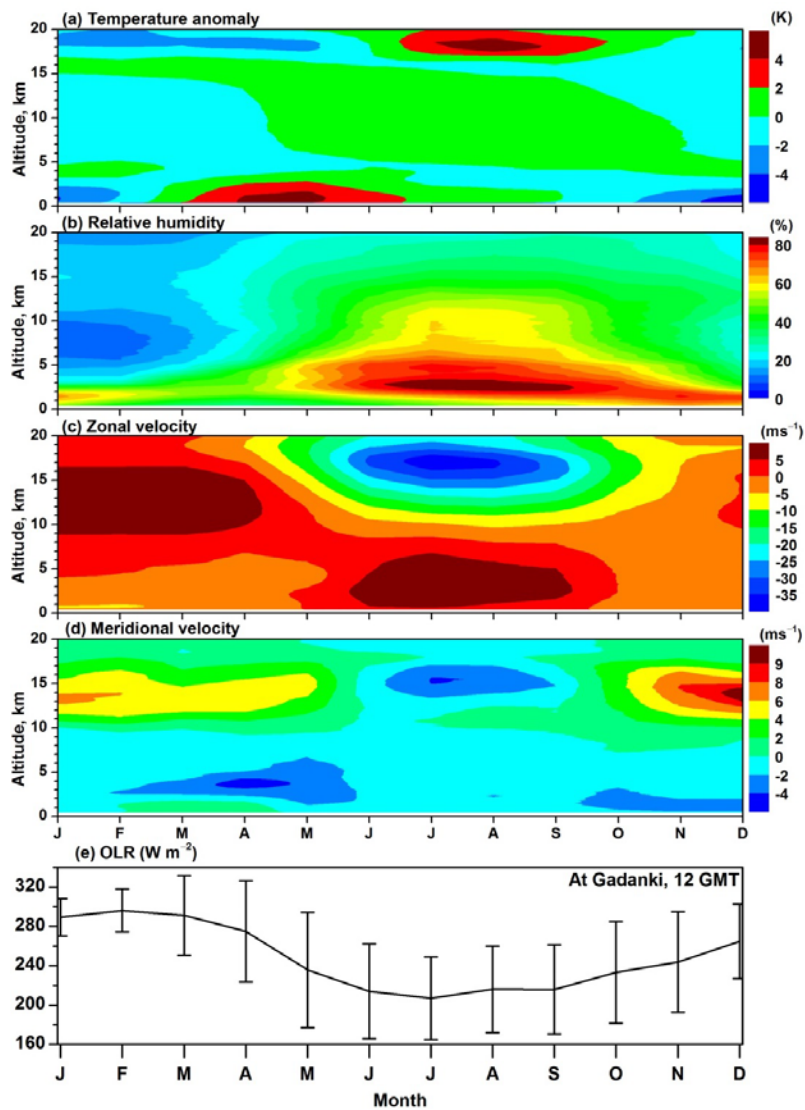


**Figure 4.** Time–altitude cross sections of monthly mean (a) Temperature anomaly, (b) Relative humidity, (c) Zonal wind and (d) Meridional wind observed over Gadanki using radiosonde observations during Apr. 2006 to May 2017. (e) Monthly mean Outgoing Longwave Radiation (OLR) over Gadanki obtained using KALPANA-1 data during Apr. 2006 to May 2017 along with standard deviation (vertical bars).

Formatted: Indent: Left: 0 cm, Hanging: 0.32 cm

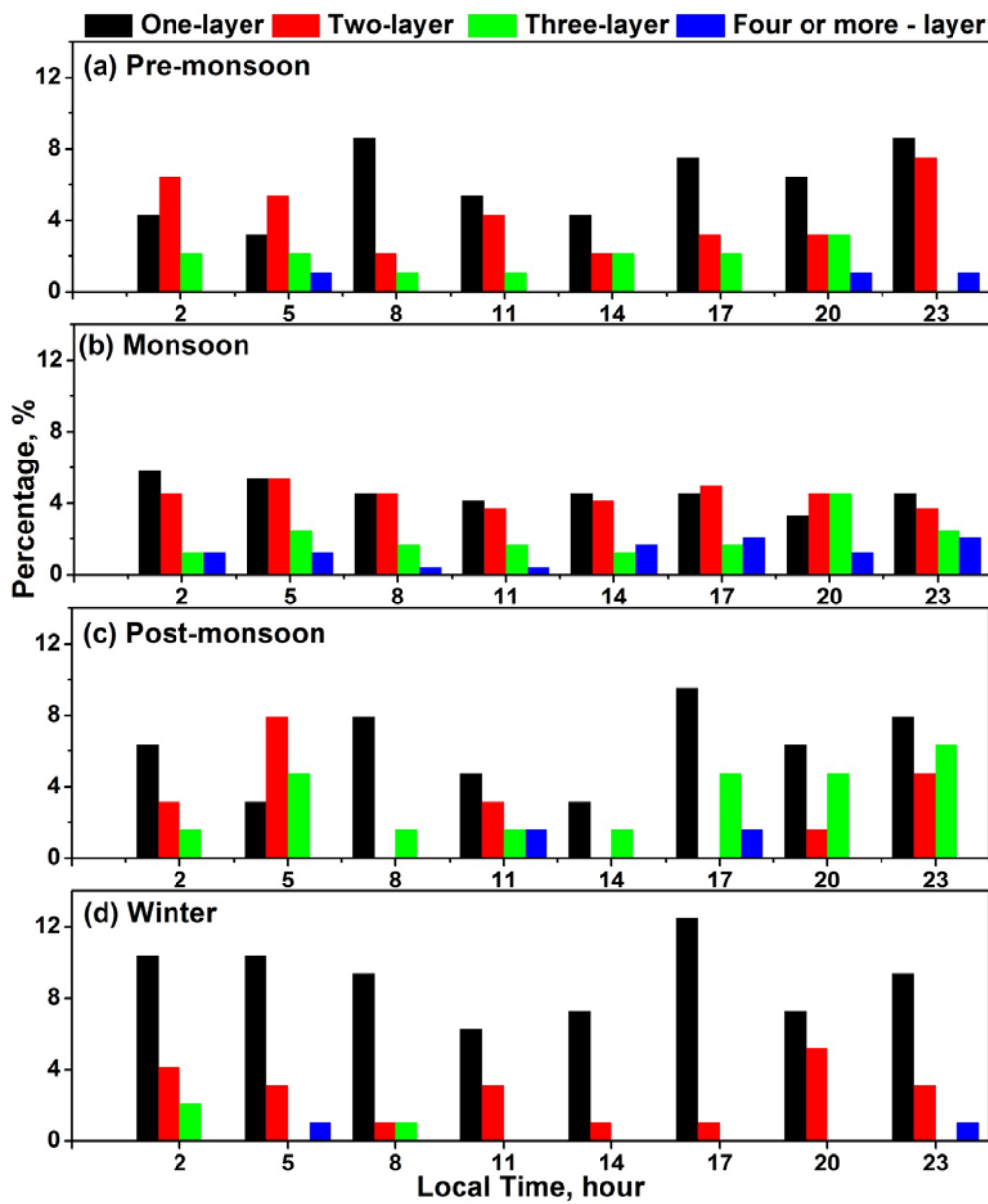


**Figure 5.** Diurnal variations of one-layer, two-layer, three-layer, and four- or more- layer clouds observed during (a) pre-monsoon, (b) monsoon, (c) post-monsoon, and (d) winter seasons.

Formatted: Indent: Left: 0 cm, Hanging: 0.32 cm

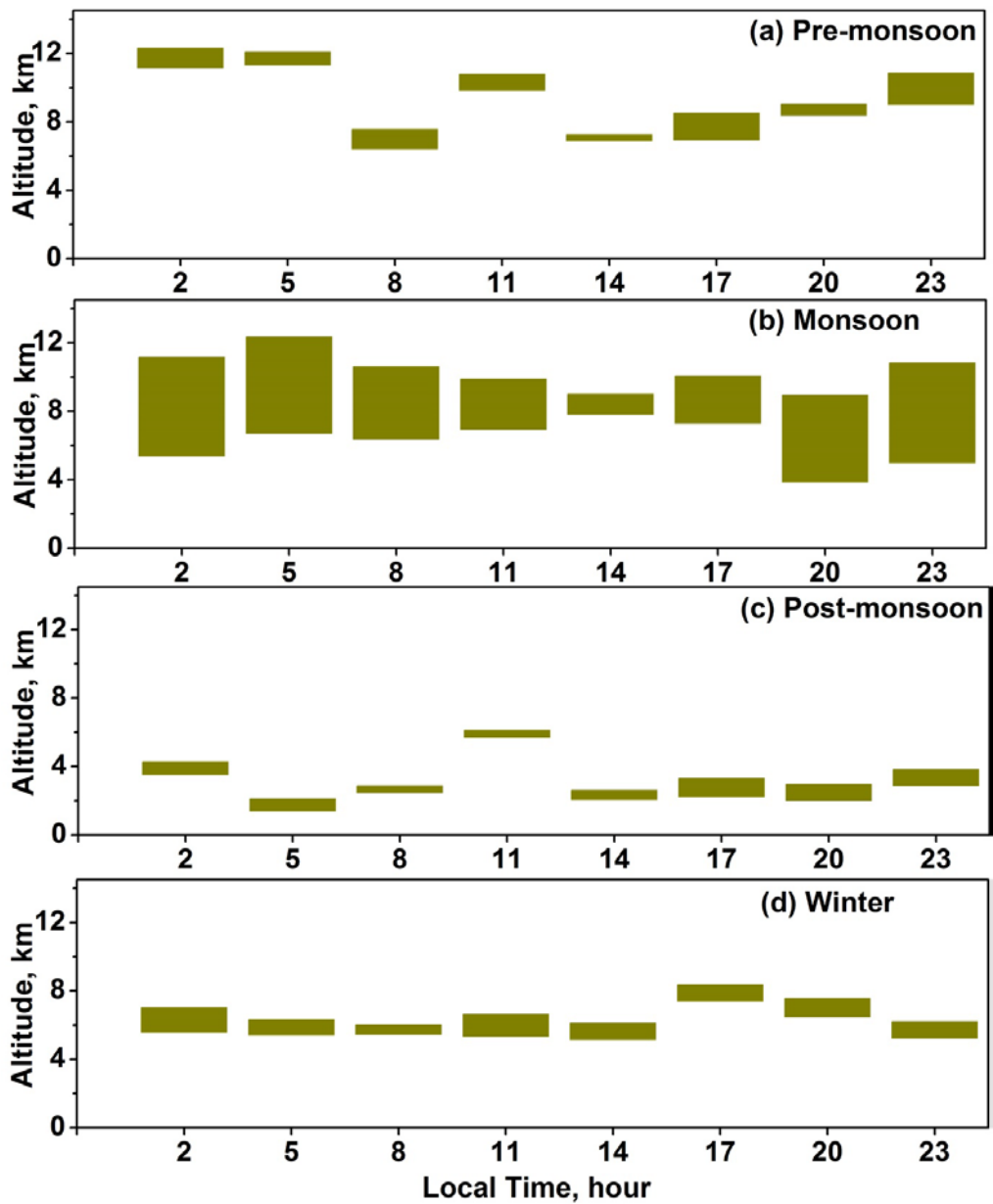


**Figure 6.** Diurnal variations of mean vertical locations (base and top), thicknesses of one-layer clouds observed during (a) pre-monsoon, (b) monsoon, (c) post-monsoon, and (d) winter seasons.

Formatted: Indent: Left: 0 cm, Hanging: 0.32 cm

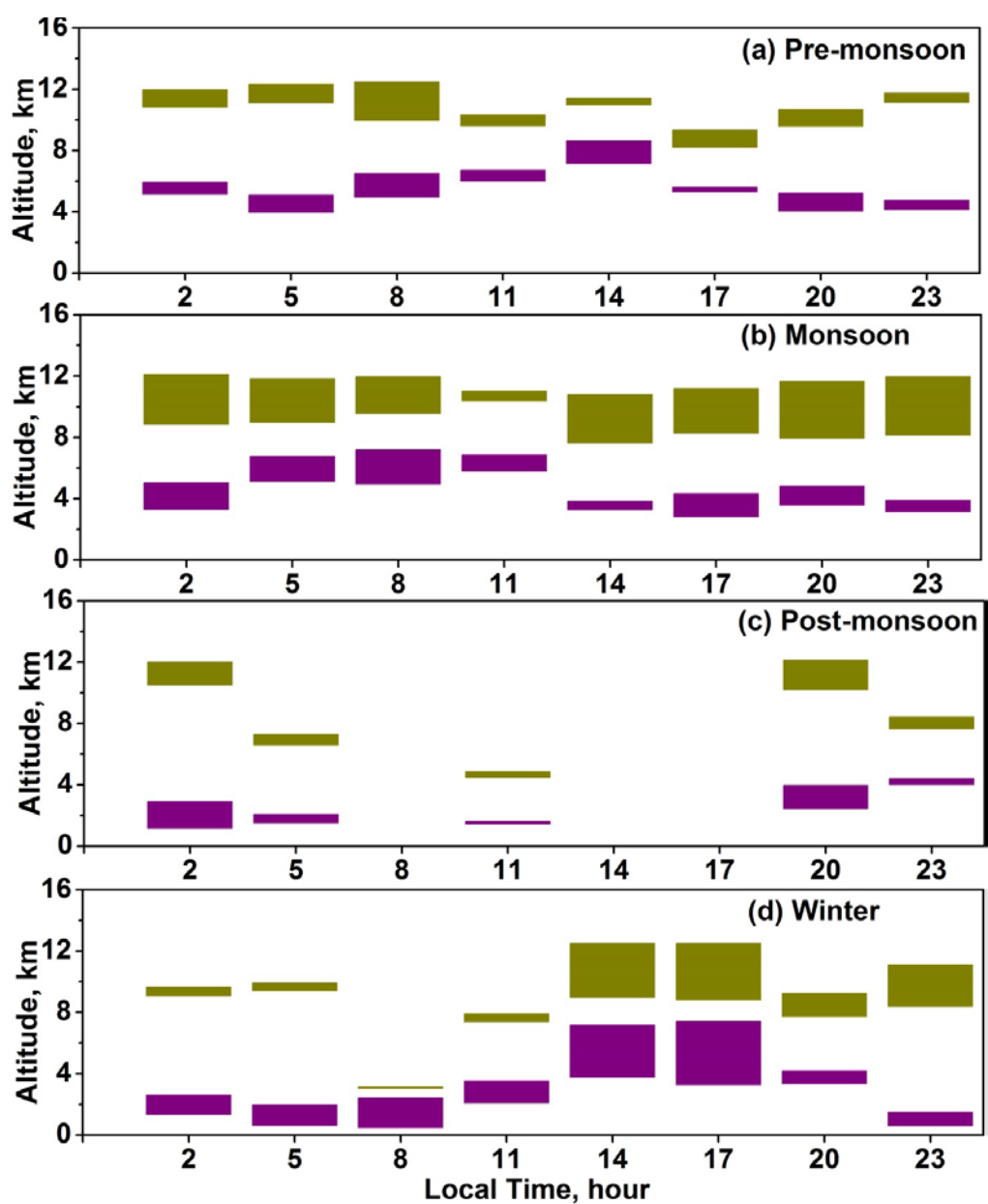
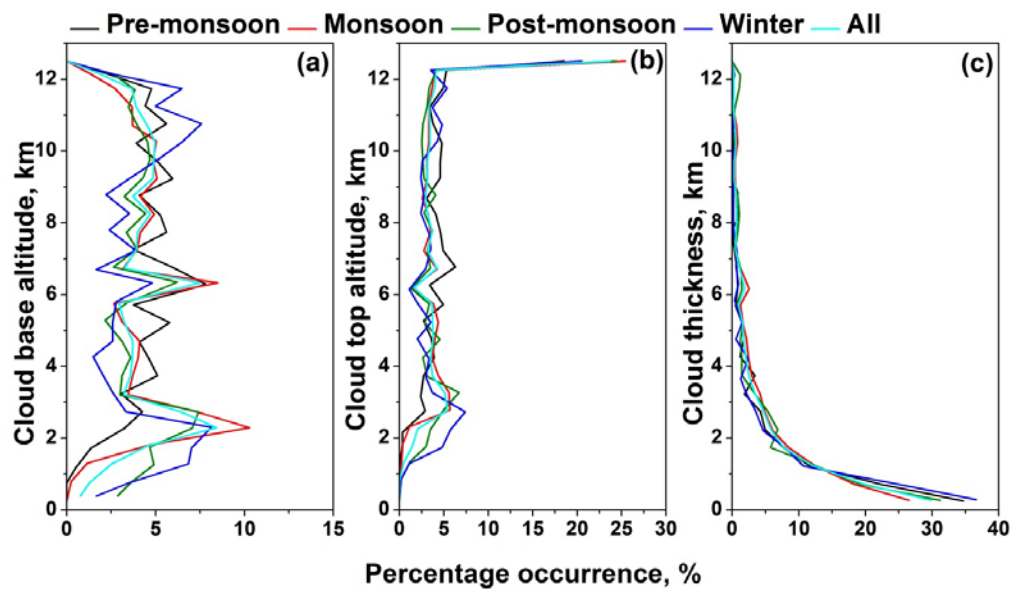


**Figure 7.** Diurnal variations of mean vertical locations (base and top), thicknesses of two-layer clouds observed during (a) pre-monsoon, (b) monsoon, (c) post-monsoon, and (d) winter seasons.

Formatted: Indent: Left: 0 cm, Hanging: 0.32 cm, Space Before: 0 pt, Line spacing: Double

1332



1333

1334 **Figure 8.**Percentage occurrence of the (a) cloud base altitude, (b) cloud top altitude and (c)  
1335 cloud thickness observed during different seasons over Gadanki. Altitude bin size is 500 m.

1336

1337

Formatted: Indent: Left: 0 cm,  
Hanging: 0.32 cm

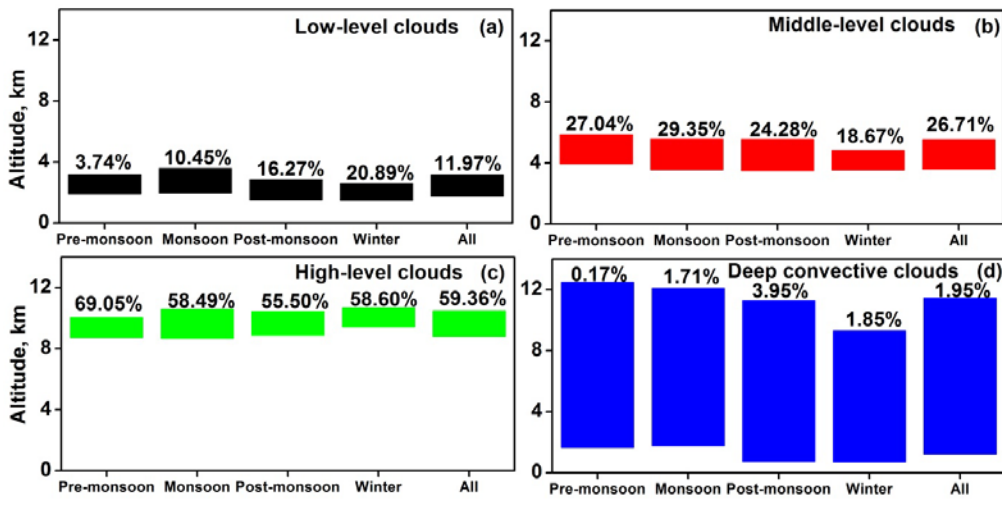


**Figure 9.** Mean vertical locations (base and top), cloud thicknesses and percentage occurrence of (a) low-level clouds, (b) middle-level clouds, (c) high-level clouds and (d) Deep convective clouds observed during different seasons.

**Formatted:** Indent: Left: 0 cm,  
Hanging: 0.32 cm



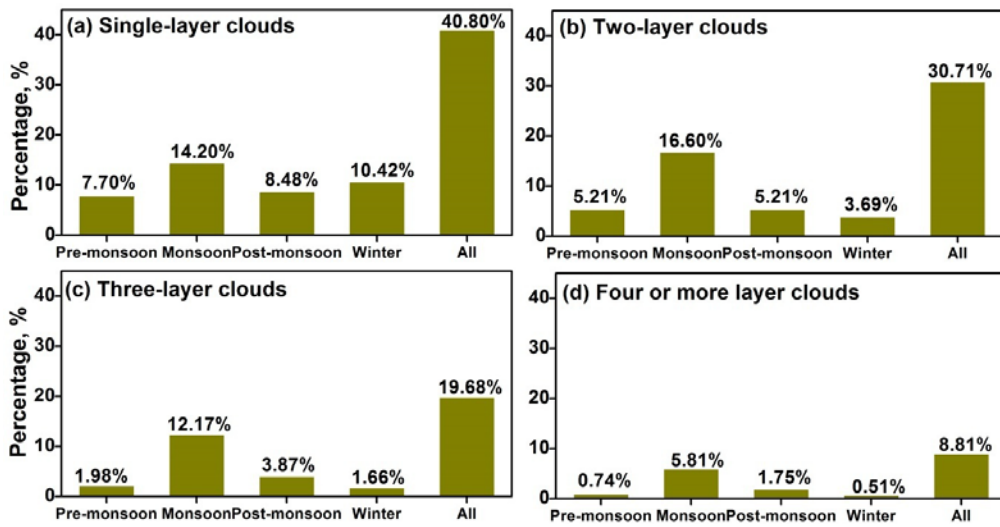


**Figure 10.** Percentage occurrence of (a) one-layer, (b) two-layer, (c) three-layer, and (d) four- or more- layer clouds observed during different seasons.

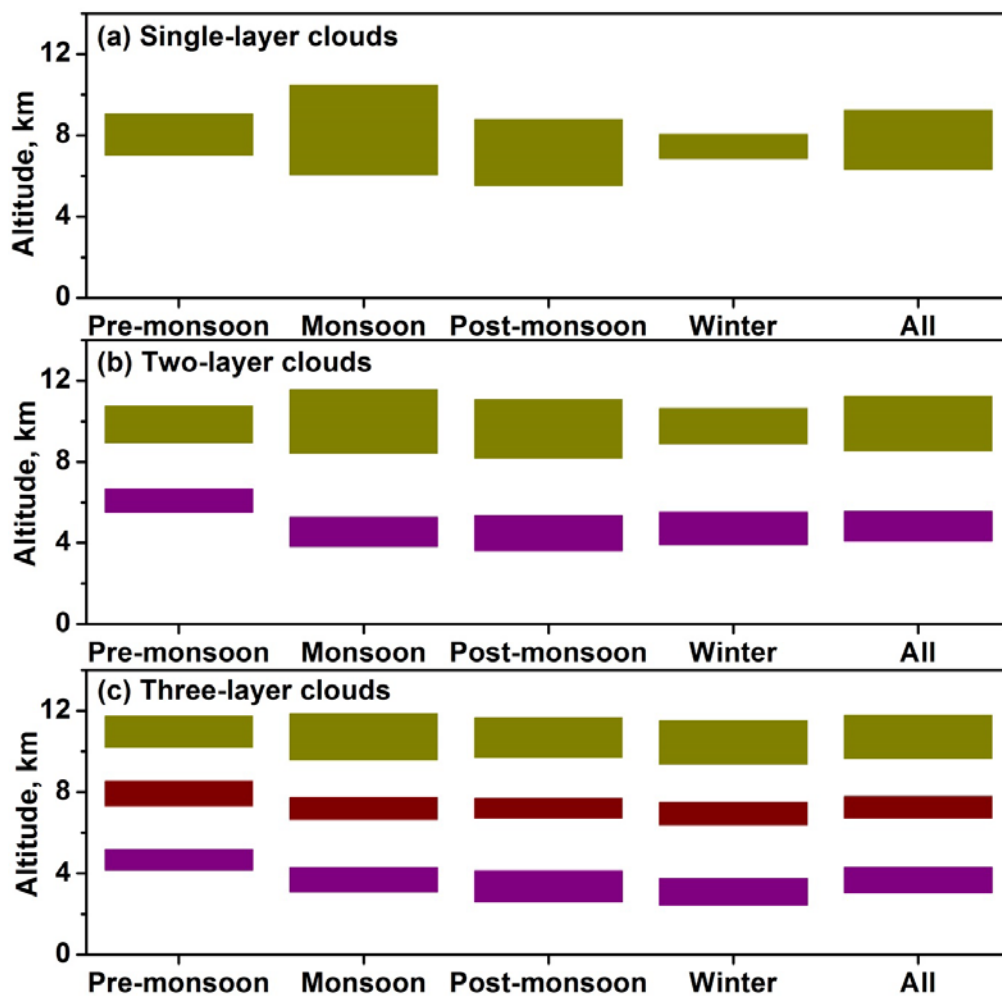


**Figure 11.** Mean vertical locations (base and top), cloud thicknesses of (a) one-layer clouds, (b) two-layer clouds, (c) three-layer clouds observed during different seasons.

Formatted: Indent: Left: 0 cm, Hanging: 0.32 cm

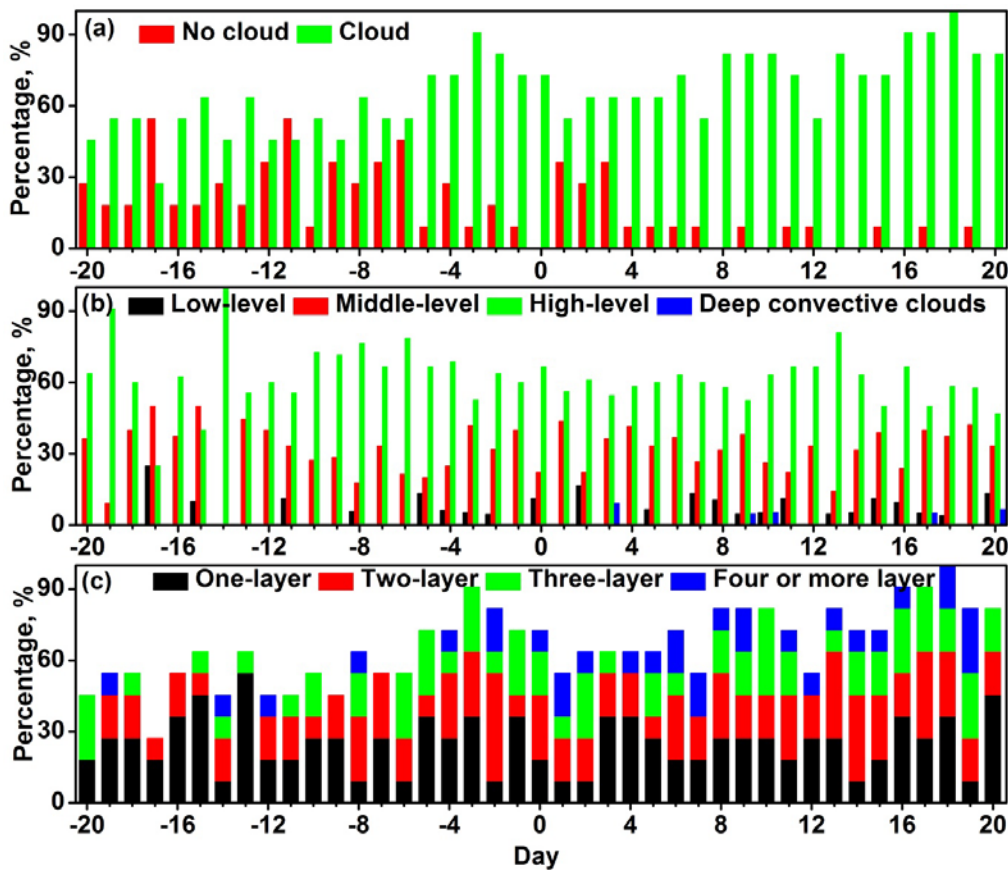


**Figure 12.** Composite (2006-2016) percentage occurrence of (a) clear and cloud conditions, (b) low-level, middle-level, high-level and deep convective cloud, and (c) one-, two-, three- and four or more- layer clouds observed with respect to the date of monsoon arrival over Gadanki location. Zero in x-axis indicates the date of monsoon arrival over Gadanki location.

Formatted: Indent: Left: 0 cm, Hanging: 0.32 cm

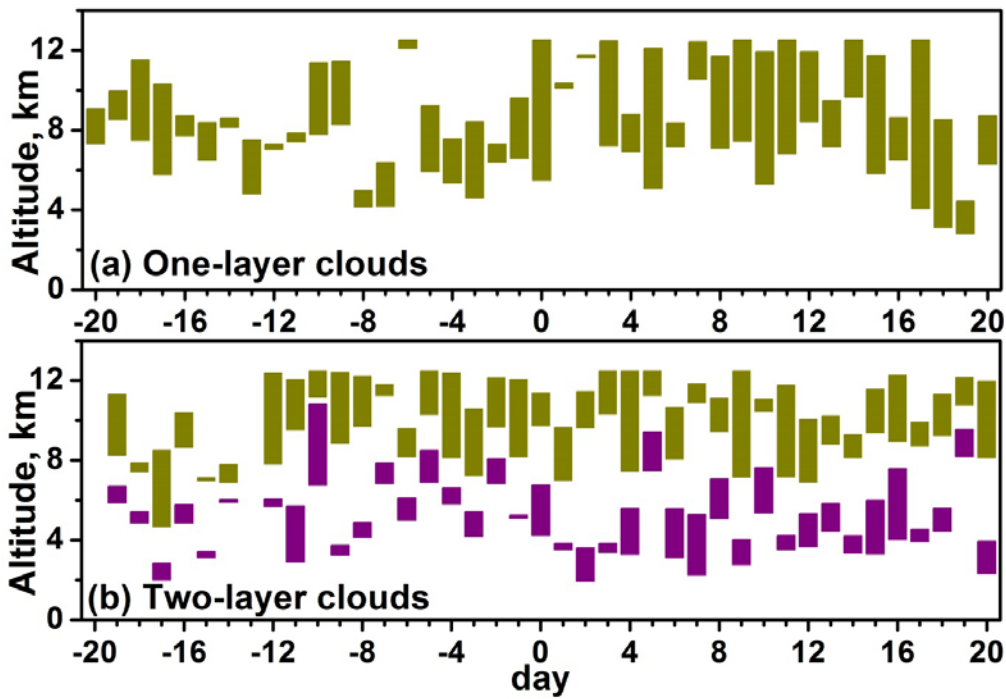


**Figure 13.** Composite (2006-2016) variations of mean vertical locations (base and top), thicknesses of one-layer clouds and two-layer clouds observed with respect to the date of monsoon arrival over Gadanki location. Zero in x-axis indicates the date of monsoon arrival over Gadanki location.

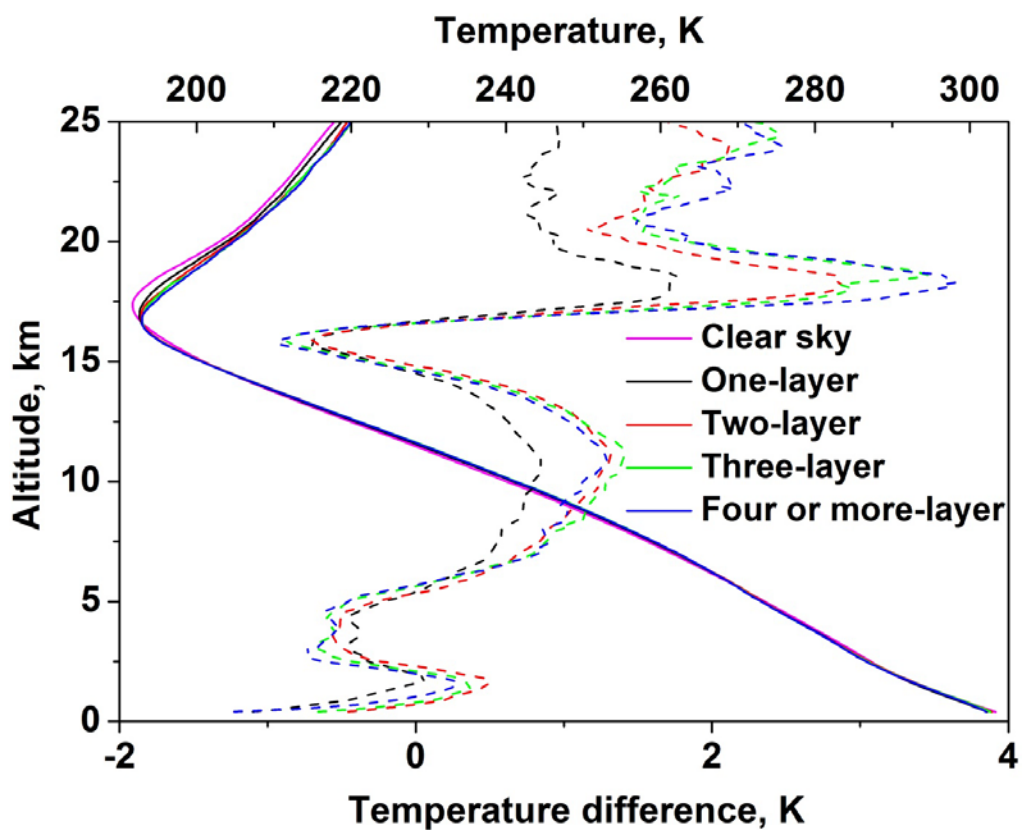
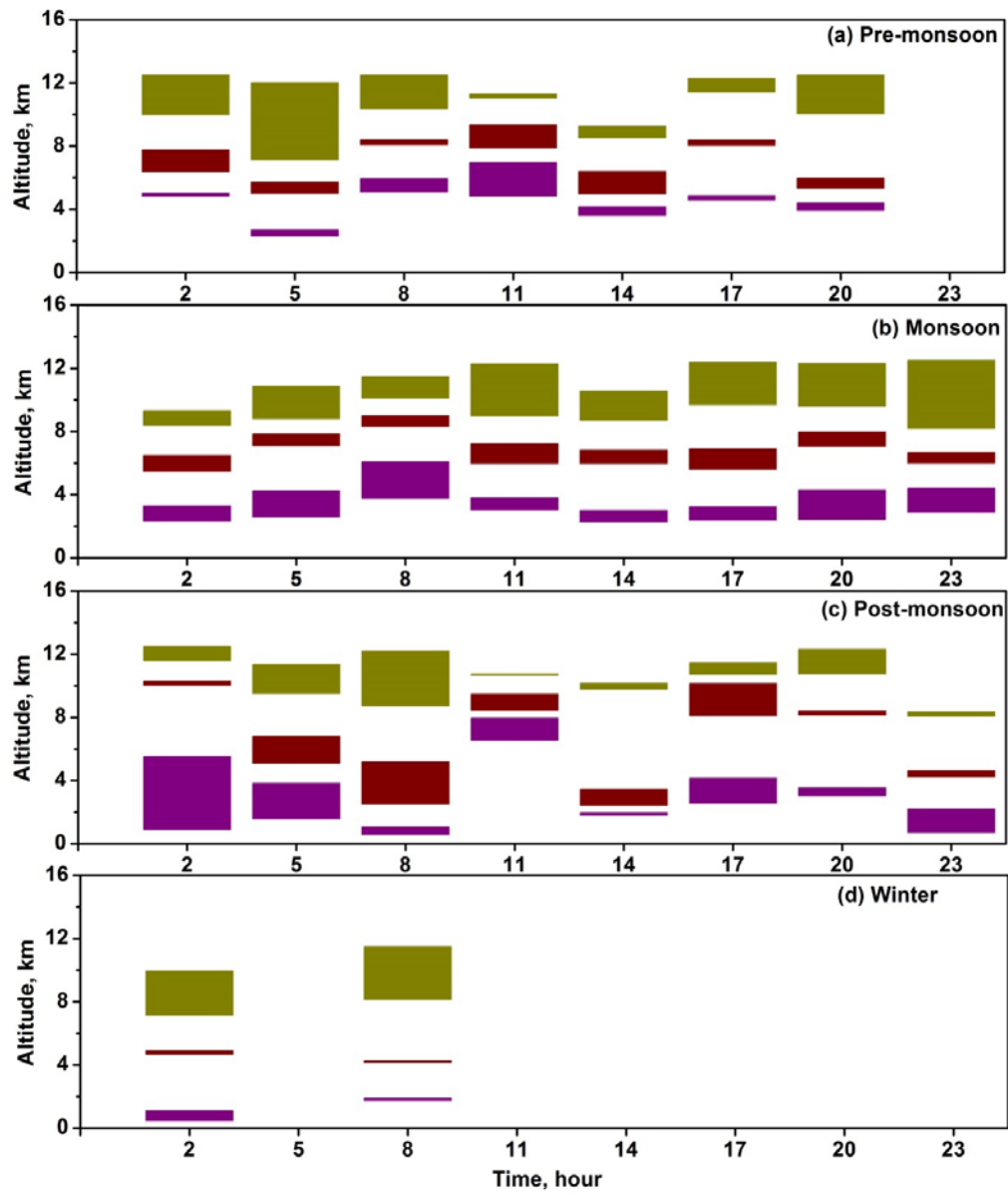


**Figure 14.** Composite (2006 – 2016) temperature profiles during clear sky, one-layer, two-layer, three-layer and four or more-layer cloud occurrences. The respective temperature difference profiles from clear sky conditions are shown with dash lines.

Formatted: Indent: Left: 0 cm, Hanging: 0.32 cm, Space Before: 0 pt, Line spacing: Double



1385  
1386 **Figure S1.** Diurnal variations of mean vertical locations (base and top), thicknesses of three-  
1387 layer clouds observed during (a) pre-monsoon, (b) monsoon, (c) post-monsoon, and (d)  
1388 winter seasons.

Formatted: Indent: Left: 0 cm,  
Hanging: 0.32 cm, Space Before: 0 pt,  
Line spacing: Double

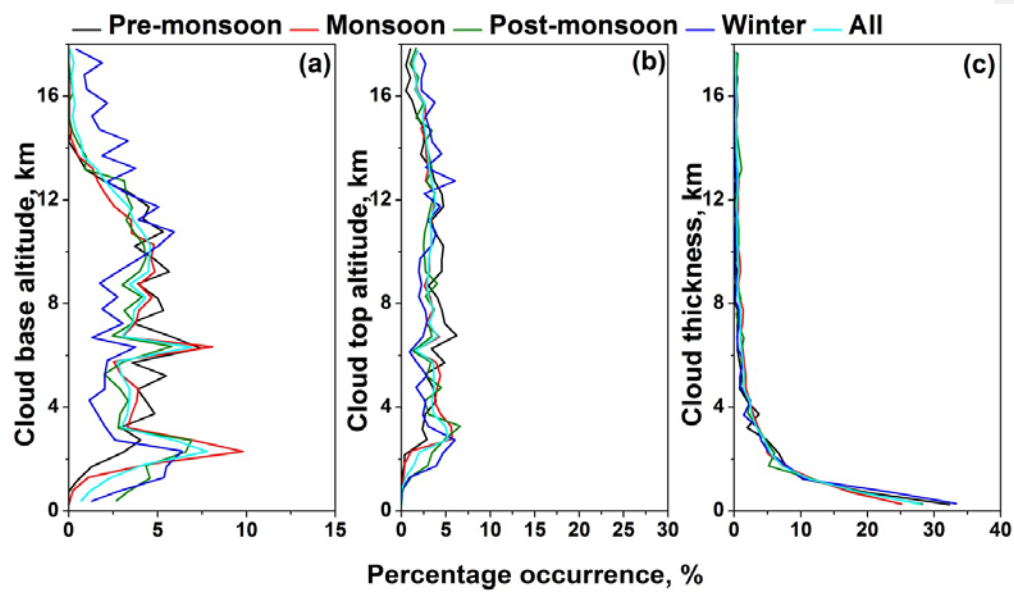


**Figure S2.**Percentage occurrence of the (a) cloud base altitude, (b) cloud top altitude and (c) cloud thickness observed during different seasons over Gadanki. Altitude bin size is 500 m.

**Formatted:** Indent: Left: 0 cm,  
Hanging: 0.32 cm, Space Before: 0 pt,  
Line spacing: Double